

## Predictive maps in rats and humans for spatial navigation

### Highlights

- We tested humans, rats, and RL agents on a novel modular maze
- Humans and rats were remarkably similar in their choice of trajectories
- Both species were most similar to agents utilizing a SR
- Humans also displayed features of model-based planning in early trials

### Authors

William de Cothi, Nils Nyberg, Eva-Maria Griesbauer, ..., Éléonore Duvelle, Caswell Barry, Hugo J. Spiers

### Correspondence

w.decothi@ucl.ac.uk (W.d.C.),  
h.spiers@ucl.ac.uk (H.J.S.)

### In brief

de Cothi et al. use a novel open-field modular maze to test the spatial navigation abilities of humans and rats, comparing them to simulated reinforcement learning agents. They find that humans and rats are remarkably similar in their choice of trajectories, with both species displaying most similarity to agents utilizing a successor representation.

Article

# Predictive maps in rats and humans for spatial navigation

William de Cothi,<sup>1,2,7,9,\*</sup> Nils Nyberg,<sup>2</sup> Eva-Maria Griesbauer,<sup>2</sup> Carole Ghanamé,<sup>2</sup> Fiona Zisch,<sup>2,3</sup> Julie M. Lefort,<sup>1</sup> Lydia Fletcher,<sup>2</sup> Coco Newton,<sup>4</sup> Sophie Renaudineau,<sup>2</sup> Daniel Bendor,<sup>2</sup> Roddy Grieves,<sup>2,5</sup> Éléonore Duvelle,<sup>2,5</sup> Caswell Barry,<sup>1,6</sup> and Hugo J. Spiers<sup>2,6,7,8,\*</sup>

<sup>1</sup>Department of Cell and Developmental Biology, University College London, London, UK

<sup>2</sup>Institute of Behavioral Neuroscience, Department of Experimental Psychology, Division of Psychology and Language Sciences, University College London, London, UK

<sup>3</sup>The Bartlett School of Architecture, University College London, London, UK

<sup>4</sup>Department of Clinical Neurosciences, University of Cambridge, Cambridge, UK

<sup>5</sup>Department of Psychological and Brain Sciences, Dartmouth College, Hanover, NH, USA

<sup>6</sup>These authors contributed equally

<sup>7</sup>Twitter: @willdecothi

<sup>8</sup>Twitter: @hugospiers

<sup>9</sup>Lead contact

\*Correspondence: [w.decothi@ucl.ac.uk](mailto:w.decothi@ucl.ac.uk) (W.d.C.), [h.spiers@ucl.ac.uk](mailto:h.spiers@ucl.ac.uk) (H.J.S.)

<https://doi.org/10.1016/j.cub.2022.06.090>

## SUMMARY

Much of our understanding of navigation comes from the study of individual species, often with specific tasks tailored to those species. Here, we provide a novel experimental and analytic framework integrating across humans, rats, and simulated reinforcement learning (RL) agents to interrogate the dynamics of behavior during spatial navigation. We developed a novel open-field navigation task (“Tartarus maze”) requiring dynamic adaptation (shortcuts and detours) to frequently changing obstructions on the path to a hidden goal. Humans and rats were remarkably similar in their trajectories. Both species showed the greatest similarity to RL agents utilizing a “successor representation,” which creates a predictive map. Humans also displayed trajectory features similar to model-based RL agents, which implemented an optimal tree-search planning procedure. Our results help refine models seeking to explain mammalian navigation in dynamic environments and highlight the utility of modeling the behavior of different species to uncover the shared mechanisms that support behavior.

## INTRODUCTION

Adapting to change is fundamental for survival. Adapting to changes in the structure of the environment has been studied in a huge diversity of psychological experiments in humans<sup>1</sup> but also more ethologically in a remarkable range of different species.<sup>2</sup> One challenge that unites all motile animals on our planet is spatial navigation. In particular, prime examples are finding a new path when a familiar route is blocked and exploiting a novel shortcut. Efficient detours and shortcuts are considered the hallmarks of a cognitive map—an internal representation of the environment that enables novel inferences to guide behavior.<sup>3–6</sup>

Both rodents and humans can show an impressive capacity to identify shortcuts and take optimal detours.<sup>5,7–17</sup> However, not all studies report successful adaptive behavior.<sup>18</sup> Rats often require multiple exposures to a set of paths before they are able to shift toward an optimal shortcut,<sup>9</sup> and may fail to select an optimal shortcut from a set of novel paths.<sup>19</sup> Humans, too, can be poor at judging the directions between locations in walled mazes, hindering the capacity to identify shortcuts.<sup>20,21</sup>

Much of the research into navigation implicitly assumes that rodents and humans navigate in a fundamentally similar way,<sup>4,22</sup> and this has been used to support the integration of insights across both species.<sup>1,5,23–26</sup> In mammals, the hippocampus is thought to form a cognitive map,<sup>25</sup> evidenced by spatially tuned cells (such as “place cells”) in the hippocampal formation of rodents and humans.<sup>27–29</sup> However, despite the wide array of human and rodent research, few experiments have sought to compare rodents and humans on a directly homologous task. Understanding the similarities and differences between these two species on the same task would be useful for allowing the better integration of findings from different methods, such as combining data from neuroimaging in humans with neural recordings and disruption methods in rodents.<sup>30–32</sup> Moreover, such integration could potentially benefit the translation of assessments in rodents to assessments for clinical trials in humans, for example, where tests of spatial navigation may be important for the early detection of Alzheimer’s disease.<sup>33–35</sup>

When considering how humans and rodents might differ during navigation, differences in sensory perception are important. Although humans have binocular vision, they may differ in olfaction<sup>36</sup> and lack the tactility of whiskers. Meanwhile, rodents have

a larger visual field of view, lower visual acuity, and can move their eyes independently.<sup>37</sup> In terms of neuroanatomy, the prefrontal cortical regions associated with spatial planning differ greatly between rodents and primates,<sup>38,39</sup> while the hippocampus and surrounding structures associated with spatial representations are relatively similar.<sup>40</sup> Given these similarities and differences, it is possible that rodents and humans navigate in a similar fashion or show pronounced differences in certain situations. Understanding such patterns in behavior is important, not only for understanding navigation but also how the behavior of different species is inter-related and may have emerged through evolutionary pressure.

One approach for identifying potential cross-species mechanisms underlying goal-directed behavior is through comparison with reinforcement learning (RL) models.<sup>41–46</sup> RL is an area of machine learning that addresses the theoretical problem of how a learner and decision maker, called an agent, should act in an environment in order to achieve a certain goal, for which it earns rewards. Specifically, the agent is not told which actions it should take but instead must learn the actions that maximize its expected future rewards, known as value. Such RL models can be used to examine how rapid learning and control can be developed in artificial systems, outcompeting human performance,<sup>41,47–49</sup> or used for comparison with patterns seen in animals or human behavior.<sup>46,50–53</sup>

Solutions to RL problems have traditionally been divided into two categories: model-based (MB) methods that afford the agent a model of the environment, used to decide actions via a planning procedure,<sup>54</sup> and model-free (MF) methods that learn from experience which actions lead to the most rewarding future.<sup>55,56</sup> Provided that the model implemented in a MB algorithm contains an accurate depiction of the environment, MB methods are typically able to respond quickly and optimally to environmental perturbations. However, the planning procedure—for example, a tree search<sup>48</sup>—required to successfully exploit the model brings with it computational complexity and overhead, particularly in large state spaces with deep transition structures, such as navigating a city.

In contrast to MB methods, MF methods are generally more simple and computationally inexpensive through a reliance on temporal-difference learning rules,<sup>55</sup> however, this comes with a reduced flexibility to environmental changes. As such, MF mechanisms are often associated with the formation of habits.<sup>57,58</sup> To achieve their simplicity, MF methods typically learn by directly estimating the value of taking a particular action in a particular state. This makes it easy to then compare the values of different actions available to the agent, without the need to know how the states are interconnected.

While MF and MB methods appear to function at opposite ends of an algorithmic spectrum, intermediary methods do exist. One such algorithm that has recently increased in application is the successor representation<sup>59</sup> (SR). The SR somewhat combines parts of MF and MB learning<sup>60,61</sup> by using experience to learn a predictive map between the states in an environment. This predictive map can be readily combined with a separately learned reward associated with each state in order to explicitly compute value. Thus, the SR negates the need for a complicated planning procedure in order to use the predictive map to guide action selection.

The SR has been able to provide a good account of behavior and hippocampal representations in humans<sup>62–66</sup> and rodents.<sup>51,67,68</sup> The tasks that are often used to draw these comparisons with RL agents typically focus on small state spaces with 2-step transition structures—as such, the extent of planning often requires one or two actions. Furthermore, due to the conceptual nature of the underlying task space, translational research usually requires differing sensory implementations for humans<sup>69</sup> and rodents.<sup>70</sup>

Here, we created a configurable open-field maze with a layout of barriers that reconfigured after a set of trials (Tartarus maze). We tested the navigation of rats in a physical instantiation of the maze, humans via an immersive head-mounted display virtual environment and RL agents in a simulation. Using a range of analytic methods, we probed how rat and human spatial behaviors compare to each other and to MF, MB, and SR reinforcement learners. We found a strong similarity in the occupancy patterns of rats and humans. Both rats and humans showed the greatest likelihood and trajectory similarity to SR-based RL agents, with humans also displaying trajectory features similar to MB-RL agents implementing an optimal planning procedure in early trials on a new maze configuration.

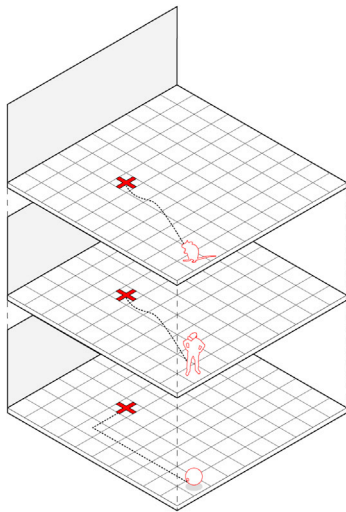
## RESULTS

Navigation was tested in a large square environment with a fixed hidden goal location and a prominent directional black wall cue in one direction (Figure 1; Videos S1—rats and S2—humans). The maze was divided into a 10 × 10 grid of moveable sections that could either be removed, leaving impassable gaps to force detour taking, or added, creating shortcuts. The speed and size of the humans in the virtual environment were set to match those of a rat traveling at 20 cm/s. During training, all 10 × 10 maze modules were present, and the rats and humans were trained to reach the goal within a 45-s time limit, (Figure 1A), while RL agents were initialized with the optimal value function. During the testing phase of the experiment, maze modules were removed to make specific maze configurations that blocked the direct route to the goal (Figure 1B). Humans (n = 18), rats (n = 9), and agents were tested on the same sequence of 25 maze configurations each with 10 trials in which a set of defined starting locations were selected to optimally probe navigation (Figure 1C). See STAR Methods for details.

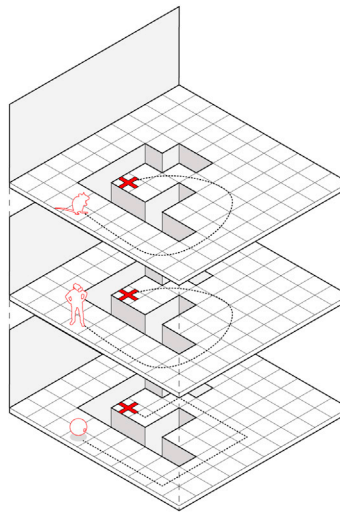
### Behavioral performance is relatively similar between rats and humans

We first asked how well humans (Figure 2A) and rodents (Figure 2B) were able to complete the task during the test sessions. As expected, repeated exposure over trials to a new maze configuration corresponded to a general increase in the ability of both the humans and rats to navigate to the goal within the 45-s time limit (Figure 2C; first 5 trials versus last 5 trials: humans  $t(17) = 6.3$ ,  $p < 0.001$ ; rats  $t(8) = 4.0$ ,  $p = 0.004$ ). Humans were also generally better than the rats at finding the goal across the 25 maze configurations (Figure 2D; humans versus rats:  $t(25) = 3.0$ ,  $p = 0.006$ ). There were 3 maze configurations in which rats outperformed humans (2, 10, and 19). We saw a strong correlation between the occupancy of the rats and human participants (occupancy correlation, humans versus rats:  $\rho = 0.67$ ; in particular, toward the later

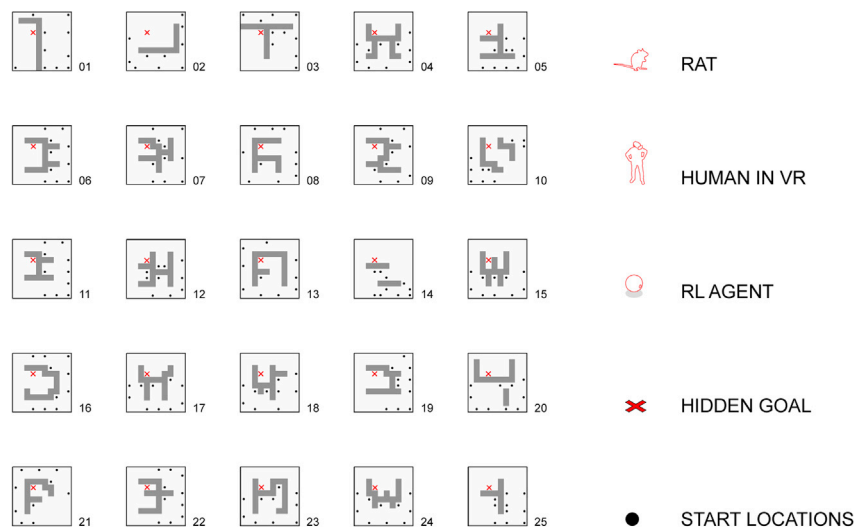
**A** Training (example trial)



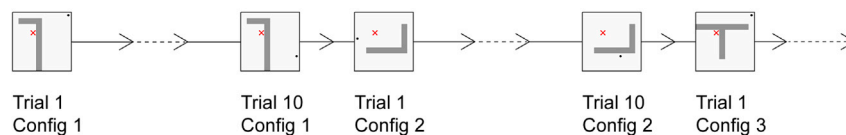
**B** Testing (example trial, maze 21)



**C** Maze Configurations



**D** Sequence of Trials



trials when both were better at navigating to the goal (Figure 2E; occupancy correlations for first 5 trials versus last 5 trials:  $t(8) = 3.2$ ,  $p = 0.013$ ). The routes used were also more efficient (Figure 2E; deviation from optimal path, first 5 trials versus last 5 trials: human  $t(17) = -5.0$ ,  $p < 0.001$ ; rats  $t(8) = -4.0$ ,  $p = 0.004$ ) with humans generally choosing more optimal routes than the rats (deviation from optimal path humans versus rats:  $t(25) = -8.2$ ,  $p < 0.001$ ). Inspection of trajectories showed that in some cases,

**Figure 1. The Tartarus maze**

(A) Schematic of the maze composed of  $10 \times 10$  units for humans, rats, and RL agents. For rats, each unit ( $20 \times 20$  cm) had a port to potentially deliver a chocolate milk reward after the rat waited 5 s at the goal (see Video S1). For humans, each unit could be associated with a hidden gold star linked to financial reward, which appeared after waiting 5 s at the goal location. Gaps between units were not visible to humans to avoid counting distance to the hidden goal (see Video S2). Example trial shows one of the possible pseudo-random starting locations on the edge of the maze.

(B) After training, flexible navigation was tested by removing units from the maze to create maze configurations with gaps between traversable surfaces. An example from maze configuration 21 is shown with one of the 10 starting locations tested. Each configuration was tested for 10 trials, with each trial having a different starting location.

(C) Sequence of 25 maze configurations used.

(D) Illustration of the trial sequence, highlighting the transition in layout every 10 trials across the 250 trials tested in the 25 maze configurations.

See also Figures S1 and S2.

near optimal paths could be observed in both species, even on the first trial of a maze configuration (see Videos S1 and S2).

**Observations of the behavior of the RL agents**

Examining the trajectories of the RL agents, we observed a number of consistent patterns.

As expected, MF agents were relatively unable to adapt to changes in the maze layout; whenever there was a barrier obstructing the learned route to the goal, the MF agent would remain in a similar region of space and often fail when the new path required traveling away from the goal or around obstacles (Video S3). This behavior logically follows from the fact that it has no representation of the transition structure and relies on previously cached optimal actions to select which transitions to make. The MB-RL agents generally chose more optimal routes, especially as the trials progressed, although they can initially be seen to occasionally make poor choices in paths

(Video S4). This is consistent with them requiring an accurate model of the environment in order to conduct a useful tree search over routes to the goal. However, when a change in the transition structure occurred and that model was no longer accurate, they do not have cached values to rely upon and must extensively explore to acquire a model of the new environment they can exploit. SR RL agents initially appear to make similar errors to MF agents but adapt more efficiently to the change

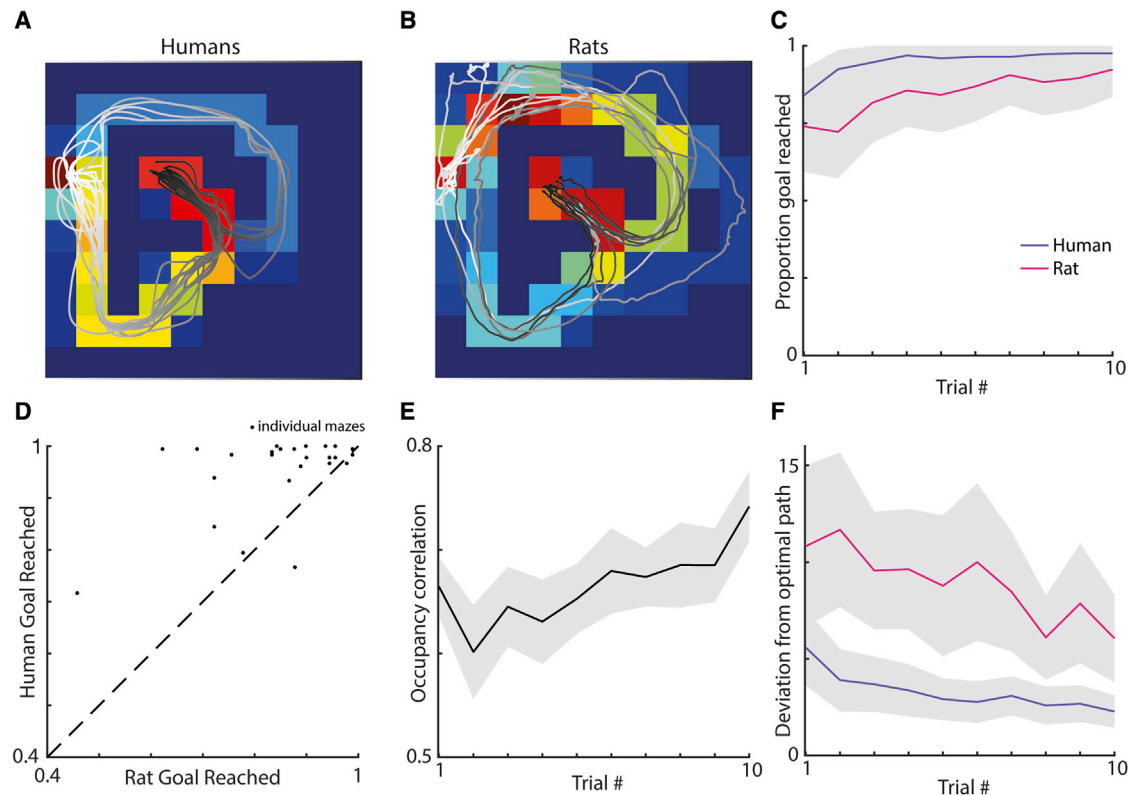


**Figure 2. Humans and rats were able to successfully navigate to the hidden goal and generally did so using similar routes**

(A and B) Examples of the human (A) and rat (B) trajectories overlaying occupancy maps for a given trial. The white-black color gradient shows the beginning-end of each trajectory.

(C) Proportion of trials where the goal was reached averaged over all configurations as a function of trial number, for rats (red) or humans (green). Gray areas indicate standard error from the mean.

(D) Proportion of goals reached by humans and rats during the time limit. The rats outperformed humans on a total of three maze configurations (2, 10, and 19), which was most pronounced for configuration 2. Configuration 1 was the configuration both species performed most inaccurately on.

(E) Correlation between the human and rat occupancy maps. Note the increase across exposure to a maze configuration, implying that they take increasingly similar routes.

(F) Average deviation from optimal path (measured in extra maze module visitations) for rats and humans as a function of trial number; humans navigate to the goal with more efficient routes.

See also [Figure S3](#).

in the transition structure, for example, avoiding dead ends after a few trials ([Video S5](#)). This is consistent with them updating a stored transition structure using past experience. Thus, unlike the MB agents, SR agents have a learned set of biases they will fall back to, which can aid choice-making after changes in the environment.

### Likelihood analysis of actions reveals that rats and humans are both most similar to an SR agent

We next investigated how the human and rat trajectories compared with the RL agents' representation of optimal actions. To do this, we computed the likelihood of the human and rat behavior matching each model by restricting the RL agents to follow the biological trajectories. We then used the internal value estimates of the agents to compute a softmax probability distribution over the available actions at each time-step. Using these probabilities to compute the likelihood of the biological data for each agent, we calculated the maximum likelihood parameter estimates for each model's learning rate

and discount factor across individual humans ([Table S1](#)) and rats ([Table S2](#)).

Comparing the MF, MB, and SR algorithms, the value representation of the SR agent consistently provided the most likely fit to the biological behavior ([Figure 3A](#); likelihood-ratio [LR] test: SR versus MF for human data  $\ln(\text{LR}) = 1,911.1$ ; SR versus MB for human data  $\ln(\text{LR}) = 538.2$ ; SR versus MF for rat data  $\ln(\text{LR}) = 842.0$ ; SR versus MB for rat data  $\ln(\text{LR}) = 225.2$ ), with the MF agent consistently providing the worst fit (MF versus MB for human data  $\ln(\text{LR}) = -1,372.9$ ; MF versus MB for rat data  $\ln(\text{LR}) = -616.9$ ). Consequently, the SR agent was the maximum likelihood model for 70% of the human trials and 60% of the rat trials ([Figure 3B](#)). Normalizing these likelihoods by trial length and using a uniform random walk as a baseline, we observed this trend was robust throughout the time spent on a maze configuration ([Figure 3C](#)) and across individuals (SR versus MF for human data:  $t(17) = 29.2$ ,  $p < 0.001$ ; SR versus MB for human data:  $t(17) = 11.9$ ,  $p < 0.001$ ; SR versus MF for rat data:  $t(8) = 13.0$ ,  $p < 0.001$ ; SR versus MB for rat

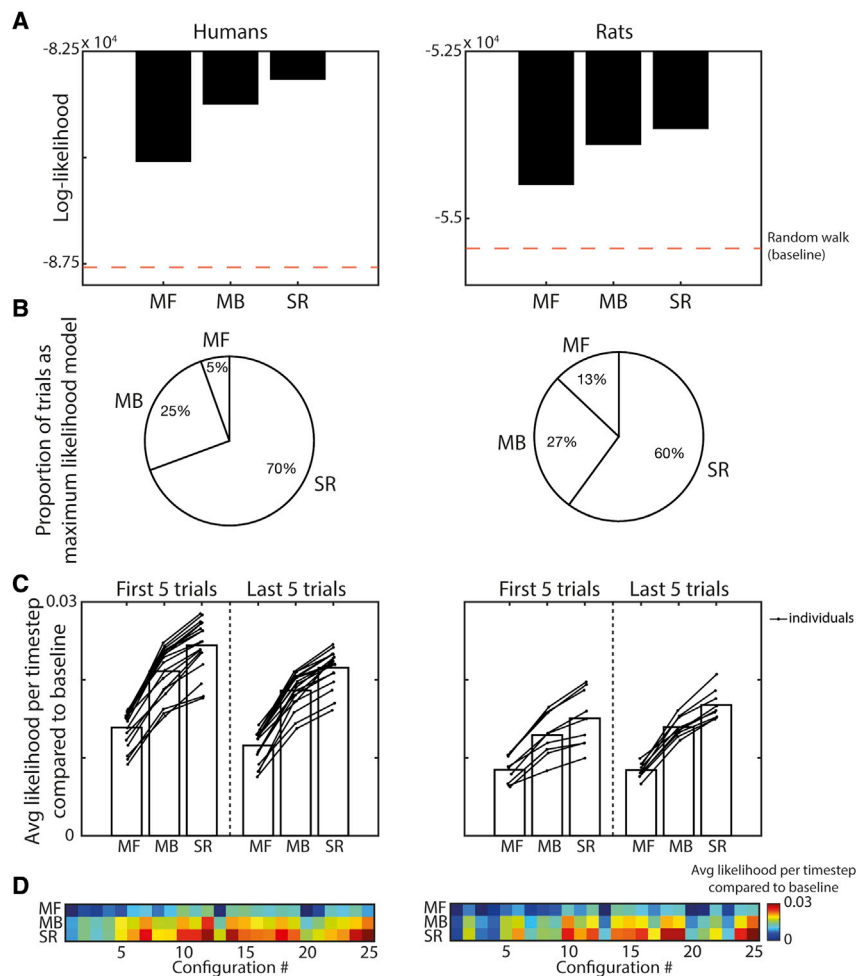


**Figure 3. Maximum likelihood analyses of the human and rat trajectories**

Likelihood analysis reveals that the behavior of humans (left) and rats (right) is better predicted by a successor representation (SR) agent than model-based (MB) or model-free (MF) agents.

(A) The value estimates generated by the SR agent provide a more likely explanation of the biological behavior than either the MF or MB agents.

(B) The SR agent was the maximum likelihood model to explain the biological behavior for the majority of trials.

(C) This trend is true across all individuals in both species (humans,  $n = 18$ ; rats,  $n = 9$ ) and robust throughout exposure to a maze configuration.

(D) Likelihood estimates vary across the maze configurations used, with a strong correlation between the model likelihoods for the human and rat behavior ( $r = 0.57$ ,  $p < 0.001$ ).

See also [Tables S1](#) and [S2](#).

data:  $t(8) = 9.6$ ,  $p < 0.001$ ). We also observed that the agent likelihoods for humans and rats varied across maze configurations ([Figure 3D](#)), with a strong correlation between the fits to the biological data ( $r = 0.57$ ,  $p < 0.001$ ).

### Simulating agents using parameters derived from the human and rat data reveal closest match to SR agent

To investigate whether these differences in agent likelihoods transfer into measurable differences in the resulting behavior, we simulated agent trajectories according to each rat and human participant, using their individual maximum likelihood parameters ([Tables S1](#) and [S2](#)). Importantly, these agents were trained on the trajectories taken by that individual on all maze configurations prior to the one being simulated. The agents then carried over all model and value representations learned across the 10 trials on the simulated maze configuration. To generate the behavior, the agents followed an  $\epsilon$ -greedy policy that linearly decayed from  $\epsilon = 0.1$  to  $\epsilon = 0.01$  across the 10 trials on a maze configuration. This means for the first trial on a new maze configuration, the agents exploit (i.e., choose the action with maximum expected value) 90% of the time and explore (i.e., choose a random action) on the remaining 10%. Then for each subsequent trial, the agents increase their proportion of time spent exploiting by 1%. To accurately depict the distribution of trajectories

generated by an agent under such a policy, we simulated each RL algorithm 100 times per rat and human participant, with the maximum number of state transitions each agent could make set to match the maximum possible for a rat traveling along the grid axes at 20 cm/s (i.e., max 45 transitions per trial, 1 transition per second). In the subsequent analyses, individual rats and human participants are compared with the RL agent simulations trained on their individual behavior, using the maximum likelihood parameters fit to their individual behavior ([Tables S1](#) and [S2](#)).

The MB algorithm generally outperformed the biological behavior ([Figures 4A](#) and [4B](#)), particularly on the first few trials of a new maze configuration (paired  $t$  test, proportion goal reached on first 5 trials: MB versus humans,  $t(17) = 2.74$ ,  $p = 0.014$ ; MB versus rats,  $t(8) = 3.20$ ,  $p = 0.013$ ; last 5 trials: MB versus humans,  $t(17) = 0.45$ ,  $p = 0.656$ ; MB versus rats,  $t(8) = 2.56$ ,  $p = 0.034$ ). The MB algorithm also consistently outperformed the other RL agents ([Figures 4A](#) and [4B](#); paired  $t$  test, proportion goal reached, human simulations: MB versus SR,  $t(17) = 22.8$ ,  $p < 0.001$ ; MB versus MF,  $t(17) = 167$ ,  $p < 0.001$ ; rat simulations: MB versus SR  $t(8) = 29.0$ ,  $p < 0.001$ , MB versus MF  $t(8) = 119$ ,  $p < 0.001$ , with the MF agent performing worst (human parameters: MF versus SR,  $t(17) = -83.8$ ,  $p < 0.001$ ; rat parameters: MF versus SR,  $t(8) = -47.0$ ,  $p < 0.001$ ). As with the humans and rats, the MB and SR agents progressively improved throughout the trials on a given maze configuration ([Figures 4A](#) and [4B](#); first 5 versus last 5 trials, human simulations: MB,  $t(17) = -40.6$ ,  $p < 0.001$ ; SR,  $t(17) = -23.6$ ,  $p < 0.001$ ; rat simulations: MB  $t(8) = -18.6$ ,  $p < 0.001$ ; SR:  $t(8) = -18.2$ ,  $p < 0.001$ ). Meanwhile, the MF agents became progressively worse at reaching the goal (first 5 versus last 5 trials: human parameters,  $t(17) = 35.8$ ,  $p < 0.001$ ; rat parameters,  $t(8) = 16.5$ ,  $p < 0.001$ ), indicative of the increasingly complex trajectories required from successive starting positions on a maze

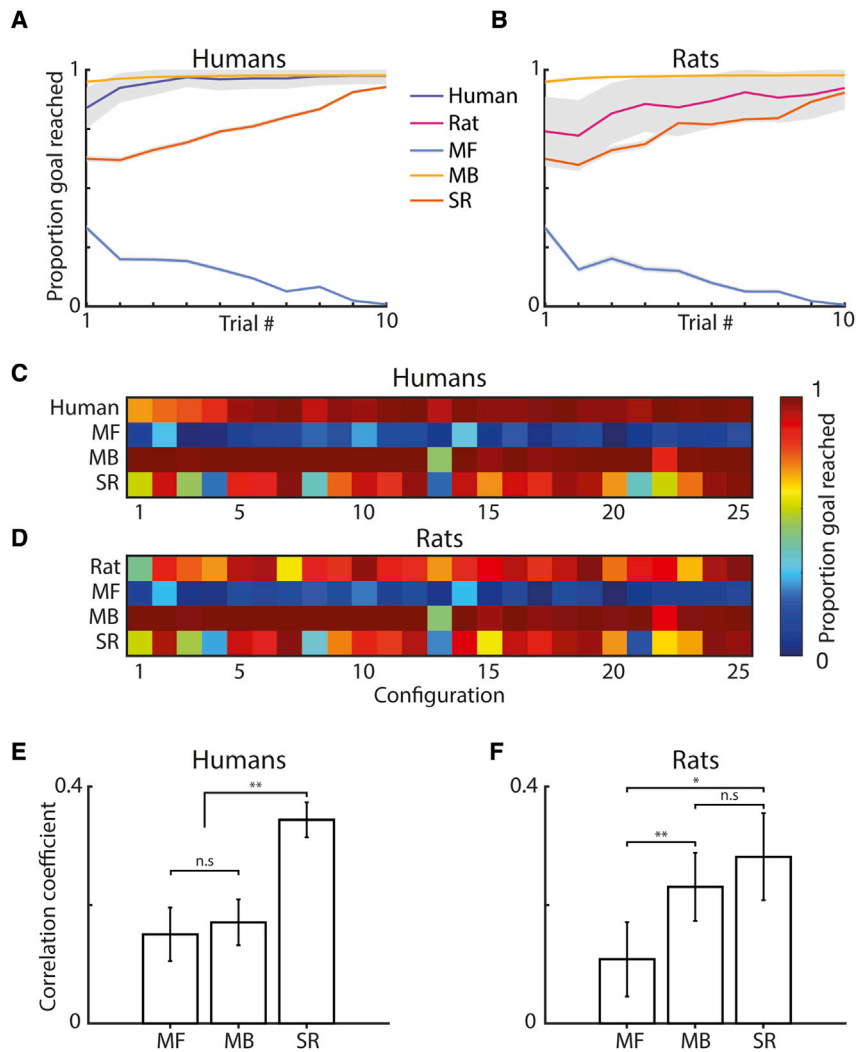


**Figure 4. Human and rat performance compared with maximum likelihood reinforcement learning agents**

(A and B) Goal reaching for agents ( $n = 100$  per participant/animal) using the maximum likelihood parameters fit to individual human (A) and rat (B) trajectories. Gray areas indicate standard error from the mean.

(C–E) (C and D) Goal reaching varied across maze configurations. Using this to rank maze configurations by difficulty reveals a significantly more positive correlation between the human and SR agent's difficulty rankings (E) than the MB or MF (paired  $t$  test following Fisher transformation: SR versus MF,  $t(17) = 3.27$ ,  $p = 0.004$ ; SR versus MB,  $t(17) = 4.57$ ,  $p < 0.001$ ; MB versus MF,  $t(17) = 0.35$ ,  $p = 0.728$ ).

(F) The rat difficulty rankings (F) correlated significantly lower with the MF agents than either of the other agents (paired  $t$  test following Fisher transformation: MF versus MB,  $t(8) = -4.33$ ,  $p = 0.002$ ; MF versus SR,  $t(8) = -2.87$ ,  $p = 0.021$ ; SR versus MB,  $t(8) = 1.00$ ,  $p = 0.345$ ). Error bars indicate standard error from the mean.

In order to establish whether the routes taken by the rats, humans, and RL agents within a maze configuration tended to follow consistent patterns of behavior, we next quantified each trajectory using diffusivity measures that were inspired by statistical mechanics and the modeling of particles moving in boxes. Specifically, for each trajectory we calculated the linear diffusivity and the sine and cosine of the angular diffusivity (Figure 5A). The linear and angular diffusivities, respectively, describe the overall directness and direction of the route, which vary from trial to trial (Figures 5B and 5C). Taken together across the entire experiment, we see that

configuration. Goal-reaching performance for the RL algorithms varied across maze configurations (Figures 4C and 4D), with configurations that had a contradictory optimal policy to the one preceding it seeming particularly difficult (e.g., configurations 4, 8, 13, and 21; see Figure 1C for specific layouts). Conversely, maze configurations that possess a high degree of coherence in optimal policy with the previous configuration (e.g., 2, 7, and 25) were consistent with higher levels of agent goal reaching due to the improved accuracy of the initial value representations. Ranking maze configuration difficulty by order of goal-reaching performance revealed a significantly more positive correlation between the human and SR agent difficulty rankings than either the MB or MF agents (Figure 4E; paired  $t$  test following Fisher transformation: SR versus MF,  $t(17) = 3.27$ ,  $p = 0.004$ ; SR versus MB,  $t(17) = 4.57$ ,  $p < 0.001$ ). Similarly, the rat difficulty rankings were significantly more correlated with those of the SR agent than the MF (Figure 4F; paired  $t$  test following Fisher transformation: SR versus MF,  $t(8) = 2.87$ ,  $p = 0.021$ ), with no significant difference to the MB agent (SR versus MB,  $t(8) = 1.00$ ,  $p = 0.345$ ).

when the trajectories are quantified this way, unsupervised clustering reveals clear patterns of behavior for each of the three RL agents (Figure 5D). Given these distinct clusters, we then used the Mahalanobis distance to measure the level of dissimilarity between the biological and agent trajectories per maze configuration. The Mahalanobis distance was used as it accounts for covariance between the diffusivity measures when calculating the dissimilarity. Using these diffusivities to quantify the general shape of the routes taken within a configuration, we found that the trajectories of the SR agents were consistently more similar to the corresponding rat and human behavior than the other agents (Figures 5E and 5F; rat simulations: SR versus MF,  $t(8) = -11.1$ ,  $p < 0.001$ ; SR versus MB,  $t(8) = -12.7$ ,  $p < 0.001$ ; human simulations: SR versus MF,  $t(17) = -55.7$ ,  $p < 0.001$ ; SR versus MB,  $t(17) = -4.21$ ,  $p < 0.001$ ). Further, the MF agent was generally the least similar to the biological behavior across the maze configurations (rat simulations: MB versus MF,  $t(8) = -2.76$ ,  $p = 0.025$ ; human simulations: MB versus MF,  $t(17) = -28.6$ ,  $p < 0.001$ ; SR versus MB,  $t(17) = -4.21$ ,  $p < 0.001$ ).

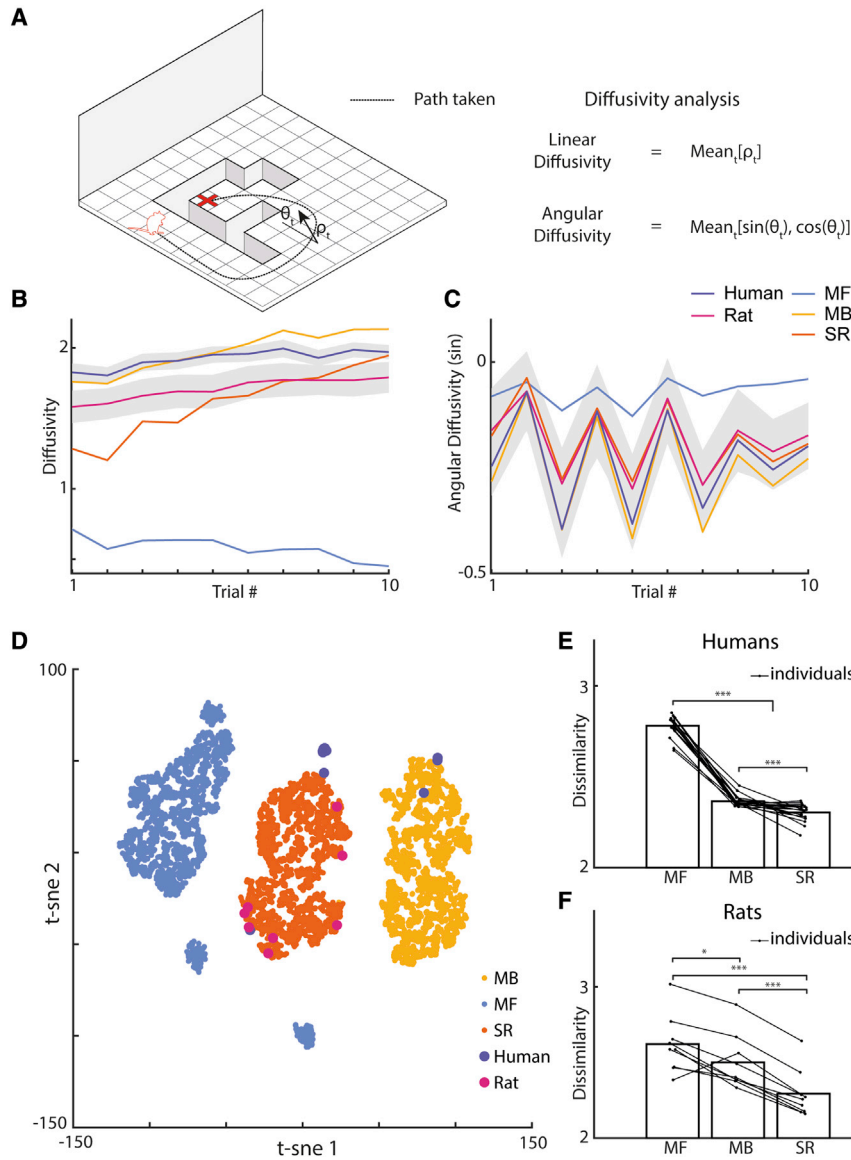


**Figure 5. Diffusivity analysis reveals rat and human trajectories are most similar to an SR agent**

(A–C) (A) Each trajectory was quantified using the average linear diffusivity (B) and the sine (C) and cosine of the average angular diffusivity. Gray areas indicate standard error from the mean.

(D) Using these metrics to quantify the trajectories on each maze configuration, agent behavior can be seen to form clusters (shown here via t-SNE), where each point represents the average of an individual human, rat, or agent over the whole experiment. Note that for different embeddings, a similar pattern emerges.

(E and F) Calculating the Mahalanobis distance between clusters reveals that the human (E) and rat (F) behavior is more similar to an SR agent than the MB or MF agents (humans: SR versus MF,  $t(17) = -55.7$ ,  $p < 0.001$ ; SR versus MB,  $t(17) = -4.21$ ,  $p < 0.001$ ; rats: SR versus MF,  $t(8) = -11.1$ ,  $p < 0.001$ ; SR versus MB,  $t(8) = -12.7$ ,  $p < 0.001$ ).

and more complex—being significantly more SR-like in both humans (Figure 6C; last 5 trials SR versus MB:  $t(17) = 8.95$ ,  $p < 0.001$ ; last 5 trials SR versus MF:  $t(17) = 33.6$ ,  $p < 0.001$ , see also Figure S4) and rats (Figure 6D; last 5 trials SR versus MB:  $t(8) = 13.4$ ,  $p < 0.001$ ; last 5 trials SR versus MF:  $t(8) = 24.8$ ,  $p < 0.001$ , see also Figure S5). Viewing how this measure of similarity changes across maze configurations again reveals noticeable variation (Figures 6E and 6F), with a strong correlation in the level of agent similarity between the rats and humans (Pearson correlation:  $\rho = 0.93$ ,  $p < 0.001$ ).

In summary, we used three approaches to compare RL agents to rats and humans: a likelihood analysis of rat and human actions under different agents; the similarity in performance between rats, humans, and RL agents trained on the biological

behavior; and the similarity of the resulting trajectories generated by these agents to the individual rats and humans on which they were fit and trained. Our results show that both species match more closely the SR RL agents' than MF or MB agents, with some features of behavior during early exposure to a new maze configuration being consistent with MB planning.

Finally, to test whether these differences in diffusivity measures across maze configurations directly translated to a physical closeness between individual trajectories, we calculated the minimum path distance between each human/rat trajectory and the simulated trajectories of the agents trained on each individual's behavior. Calculating this at every state along a human/rat trajectory and averaging across the length of the trajectory gives a measure of similarity between the biological and agent routes taken. We see that the SR agent trajectories are generally closer to both the human (Figure 6A; SR versus MB:  $t(17) = 8.32$ ,  $p < 0.001$  SR versus MF:  $t(17) = 28.8$ ,  $p < 0.001$ ) and rat paths (Figure 6B; SR versus MB:  $t(8) = 6.44$ ,  $p < 0.001$ ; SR versus MF:  $t(17) = 26.4$ ,  $p < 0.001$ ). Interestingly, humans displayed evidence of MB planning on the early trials of a new maze configuration (Figure 6C; first 5 trials MB versus SR:  $t(17) = 3.30$ ,  $p = 0.004$ ; first 5 trials MB versus MF:  $t(17) = 17.0$ ,  $p < 0.001$ ), with the latter half of trials—when the routes to the goal were longer

behavior; and the similarity of the resulting trajectories generated by these agents to the individual rats and humans on which they were fit and trained. Our results show that both species match more closely the SR RL agents' than MF or MB agents, with some features of behavior during early exposure to a new maze configuration being consistent with MB planning.

## DISCUSSION

To understand the underlying processes that support flexible navigation in rats and humans, we compared their navigation performance with three classic instantiations of RL agents in a maze environment using a dynamic layout of barriers. Using a combination of likelihood, performance, and trajectory similarity analyses, we find that both rats and humans rapidly adapted to the dynamic environments, producing similar navigation choices and trajectory patterns that most resembled



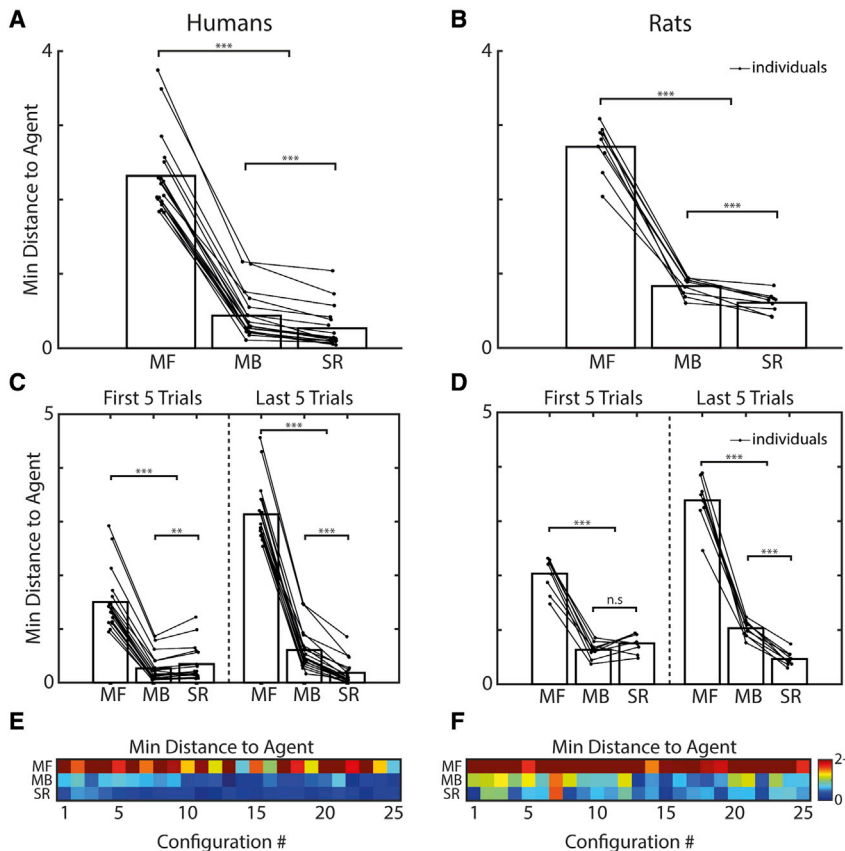


**Figure 6. Trajectory similarity analysis identifies SR agent trajectories as closest to human and rat behavior**

Trajectory similarity to the MF, MB, and SR agents was measured using the average minimum path distance along each human (left column) and rat (right column) trajectory.

(A) SR agent trajectories were in general closest to both the human (SR versus MB:  $t(17) = 8.32$ ,  $p < 0.001$  SR versus MF:  $t(17) = 28.8$ ,  $p < 0.001$ ) and (B) rat behavior (SR versus MB:  $t(8) = 6.44$ ,  $p < 0.001$ ; SR versus MF:  $t(17) = 26.4$ ,  $p < 0.001$ ), although (C) humans displayed evidence of MB planning in early trials on a new maze configuration (first 5 trials on a configuration, MB versus SR:  $t(17) = 3.30$ ,  $p = 0.004$ ; MB versus MF:  $t(17) = 17.0$ ,  $p < 0.001$ ) and (D) rat data (last 5 trials on a configuration SR versus MB:  $t(8) = 13.4$ ,  $p < 0.001$ ; SR versus MF:  $t(8) = 24.8$ ,  $p < 0.001$ ). The level of similarity to agent trajectories varied across maze configurations (E and F) with a strong correlation between the humans and rats (Pearson correlation between both matrices:  $\rho = 0.93$ ,  $p < 0.001$ ).

See also [Figures S4](#) and [S5](#).

SR RL agents. This was most evident for rats, although humans were also found to show some trajectory patterns similar to MB-RL agents in early trials. Our findings provide novel convergent cross-species insights into spatial navigation behavior and mechanistic understanding of the different choices made when adapting to a changing environment. In doing so, we identified a set of metrics that could allow the prediction of future behavioral and neural dynamics across a wide range of methods in humans and animals. We discuss: (1) how these results inform our understanding of mammalian navigation, (2) insights into RL models, (3) similarities and differences between rodent and human behavior, and (4) directions for future research.

### A predictive map for navigation?

Naively, one might view rats as “creatures of habit,” while humans could be considered deep thinkers, mulling over future possibilities. These two stereotypes map, to some degree, onto MF RL (habit-like) agents and MB-RL (flexible planning) agents. Rather than finding such a dichotomy between rats and humans, we found that the behavior of both species is best captured by an RL agent that creates a predictive map of the environment to guide navigation: the SR. The SR has been proposed as an efficient alternative to the relatively inflexible MF RL and the computationally expensive MB-RL. SR stores a matrix of the possible transitions within the environment and integrates this with information about reward.<sup>59</sup> Recently, it has been proposed that the hippocampus may implement a system

similar to a SR to create a predictive map to guide navigation.<sup>67,68,71,72</sup> Here, we find behavioral evidence to support the proposal that both rats and humans use such a predictive map to guide flexible navigation behavior. This match of the rodent behavior to SR agents is consistent with evidence that rats can carefully evaluate different options for navigation.<sup>73</sup>

A range of previous experiments comparing human behavior to RL agents has generally focused on a competition of MF versus MB agents to capture behaviors in small conceptual state spaces with 2-step transitions. These have found evidence for MB planning in humans.<sup>69,74,75</sup> Using a much larger state space with the potential for recursive transitions (i.e., loops leading back to the same state), we extend this approach into a more complex and naturalistic framework. Our findings add to recent evidence that the choices of humans are best explained by a combination of SR and MB behaviors.<sup>64–66</sup> Because the SR encodes the environment’s transition structure, it is itself a transition model that can be leveraged for intuitive planning<sup>76</sup> or more explicit planning procedures, such as a tree search, which may partially explain trajectories observed during hippocampal replay.<sup>24,45,77–80</sup> Given that the MB learner will generally improve the accuracy of its learned model as it has more experience of a maze layout, it might be surprising that we observed a greater match to SR agents during the second half of trials on a new maze configuration. However, the MB planning mechanism of simulating possible future paths is considerably more resource-intensive than drawing upon a cached knowledge of past behaviors gleaned from experience. Thus, for a metabolically constrained learning system, it would be more efficient to fall back on simpler processing mechanisms when they

reach a certain threshold in terms of performance (e.g., maximizing reward and/or minimizing uncertainty in an expected reward), which is supported by evidence in both rodents and humans.<sup>51,81</sup>

A few studies have explored human navigation in virtual reality (VR) environments and compared navigational choices with RL agents, reporting that the behavior matches a mix of MB and MF choices.<sup>46,50</sup> For example, when paths are short but decision times are longer, MB-RL agents were found to better match human behavior.<sup>50</sup> However, these past studies did not compare performance with a SR, nor were the trajectories examined in relation to metrics such as diffusivity and physical closeness to understand the match to different RL agents. Here, we show that navigation in humans is most similar to SR and that using trajectory information is useful in providing convergent evidence to understand this.

In our experiment, the MF RL agents showed poor adaptation to the changes in maze layout. Rather than improving over trials, performance declined. This could be accounted for by our task structure; the minimum trajectory length increased as trials progressed, requiring longer and more complex routes to the goal. Our maze configurations were designed to be simple but to include dead-end zones and/or regions where the barriers extended around the goal zone, requiring extended trajectories away from the goal to then reach it. It is possible that with different layouts MF learners would succeed more efficiently. Understanding how the structure of the task and state space leads to the emergence of different policies is an important question for future research.

A key observation in our data is that it is not sufficient to conclude on the basis of overall performance which simulated agents will best fit the biological agent's data. Although the MB-RL agent performed best and was closest overall to the human performance, the SR RL model produced the greatest match in terms of the proportion of trials as the maximum likelihood model. This is because the patterns of choices made by the MB-RL fail to capture aspects of choice and trajectory patterns in the rats and humans to the same degree as the SR agents. This highlights the utility of an environment in which a wide diversity of trajectories can be achieved by the rats and humans to allow models to be discriminated.

### Similarities and differences in the flexible behavior of rats and humans

Past research has suggested that rats do not always optimally adapt to selecting appropriate alternative routes when navigating<sup>9</sup> and can take time to adjust to such changes to select the optimal route.<sup>14,82</sup> Similarly, humans can struggle to take optimal shortcuts when presented with options.<sup>8,20,21</sup> Here, rats and humans had to reach the correct goal from a set of 100 possible locations within a 45-s time limit. Because the maze transition structure was reconfigured every 10 trials, achieving this was non-trivial. Despite this, both species were able to reach the goal on the first trial of a new layout on many maze configurations. This parallels recent evidence from mice learning new paths remarkably fast in a large labyrinth.<sup>83</sup> In several cases, we saw examples of routes near the optimal path on the first attempt for both species (e.g., see [Videos S1](#) and [S2](#)). Moreover, the occupancy correlation between rats

and humans was relatively high—even from the first trial—and improved as performance increased across trials in a configuration. These results show that our Tartarus maze, with its visual access to landmarks, boundary geometry, and canyon-styled barriers, provides a useful assay for goal-directed navigation across two species, revealing a remarkable similarity in the patterns of navigation across species.

Despite similarities in behavior, there were noticeable differences between species. Humans were more successful at adapting to the changes in maze layout and learning, while rats spent more time on the perimeter of the maze's edge. The overall difference in learning likely relates to the physical differences in our maze used between rats and humans (real versus VR<sup>84</sup>) and the biological differences between species (e.g., differences in vision, movement, whisking, olfaction, grooming, and predator/prey status). The current models assume that optimal routes minimize distance. However, rats will also need to avoid predators, thus selecting certain routes that are safer may also drive route choice.<sup>14</sup> Rats also need to find suitable and safe places to groom their fur. These factors may underlie the generally poorer fit of the models to rats than humans. Additionally, while fog was used in the human VR to better match the visual acuity and depth perception between rodents and humans,<sup>85</sup> the rats had visual access to more of the maze during the experiment—with recent evidence in humans suggesting that this can bias strategies toward an SR.<sup>53</sup> Further research would be needed to disentangle the various contributions that give rise to the differences we observed.

### Benefits of a dynamic open-field environment with barriers

Prior studies examining navigation in mazes have generally either used track-based or open-field environments.<sup>29,86,87</sup> Although open-field environments place more demands on self-localization and vector-based navigation,<sup>79,88,89</sup> mazes with tracks enable testing of the effects of blocked paths and shortcut behaviors.<sup>6,9,82,86</sup> By contrast, the Tartarus maze places demands on both vector-based navigation and the capacity to take detours and shortcuts, as occurs with much of the terrain in the real world. The recent development of the honeycomb maze for rats<sup>90</sup> provides a parallel approach to self-localization and obstructed paths to goals, where rats sequentially navigate to a goal over a number of hexagonal platforms that are made available in pairs until the goal platform is reached. Such an approach allows for a precise assessment of choice options at different time points, while placing demands on self-localization in relation to distal cues. Although the Tartarus maze also demands choices and navigation to distal cues, it allows continual, often ballistic, trajectories to be taken to the goal, mimicking naturalistic behaviors that enable integration with more ethological approaches to navigation.<sup>91</sup>

A number of rodent studies have examined how maze layout and changes in layout relate to exploration behavior<sup>83,92–96</sup> or escape behavior.<sup>14,97</sup> Here, we found that rats and humans rapidly adapted to changes in the maze structure by exploring the new layout. By matching to RL models, it is possible to provide a more mechanistic account of how goal-directed behavior is organized during the navigation of a dynamic environment. In the case of Rosenberg et al.,<sup>83</sup> mice had to learn the paths in a

maze with a large number of options. Akin to our task, learning was rapid. This differs from many non-spatial learning tasks where learning is typically slow (see Rosenberg et al.<sup>83</sup>). Other recent rodent studies exploring navigation behavior have shown the capacity to model behavior in goal learning and homing vectors for safety.<sup>14,89,96,98</sup> Such studies highlight the value in modeling to understand the mechanisms guiding behavior. Here, we demonstrate the added benefit of modeling behavior with simulated agents, examining the trajectory properties (e.g., diffusivity) and comparing across two different species. Across many studies distal cues are kept constant allowing for rapid learning of the new layout. Manipulating these distal cues would be an interesting direction for future research.

Prior human virtual navigation studies exploring flexible navigation behavior have tended to involve complicated VR environments that would likely be too demanding for rodents to learn.<sup>10,12,13,21,46,53,99,100</sup> Here, we sought to recreate an environment that would challenge human participants generating sufficient variation in performance and to allow comparison to rodents within the same maze structure. Being able to integrate behavioral data from humans, rodents, and RL agents, opens the possibilities for incorporating data from a wide array of neuroscience methods in humans and rodents. Recent studies have shown the utility of this approach.<sup>30–32</sup> A study by Zhu et al.<sup>53</sup> highlights the benefit of examining eye-movement dynamics during the navigation of virtual environments, using a similar head-mounted display to our human VR, but where the whole transition structure was visible to look at. Their results show patterns of eye-movements that sweep across key points in mazes, maximally important for planning, showing forward sweeps to the goal as well as backward sweeps from the goal. Furthermore, they show evidence that patterns in eye-movements that scan relevant available transitions relate to SR agent performance. Future work with eye-tracking integrated into our human task would be useful to study the selection of sub-goals and eye-movements after changing the maze layout; could eye-movements predict future choices of route and the match to different RL agents in subsequent behavior? Eye-tracking in rodents is a bigger challenge but may also hold some promise.<sup>101</sup> Finally, it may also be useful to explore the search behavior of RL agents, humans, and rats in relation to models of utility and biased search.<sup>102</sup> Such explorations would be interesting to examine in mazes ranging in complexity, visibility (fog-levels), and frequency of re-configuration. Based on our results, we would predict that human behavior would match MB agents more in rapidly changing environments and environments where they can see more of a complex layout that would benefit from deliberating over the options.

### How might the RL agents be improved?

The learning efficiency of RL agents could be improved using offline replay of randomly sampled past experiences.<sup>45,61,65,103</sup> These replays are typically implemented between agent time-steps, and the manner in which they are sampled can further accelerate learning by prioritizing the most useful learning experiences to replay.<sup>77</sup> Prioritized replay also has strong parallels with the phenomenon of hippocampal replay of place-cell activity during sleep or quiescence.<sup>79,104,105</sup> However, in this study we did not implement agent replay in order to keep the value

representations, and consequently the likelihoods of agents, deterministic. An alternative way to improve the goal reaching of agents could be through improving their exploration policy. The agents simulated here relied on an  $\epsilon$ -greedy policy through which exploration is driven purely by chance. However, methods that include curiosity<sup>106</sup> or uncertainty in the value function<sup>107,108</sup> could be used to guide more efficient exploration of a new maze configuration and consequently lead to faster learning. Finally, navigation using an options-framework might allow for more efficient navigation;<sup>109</sup> rather than planning step by step, efficient navigation in our maze configurations can be achieved by selecting a clockwise versus counter-clockwise path to the goal. Being able to exploit a hierarchical segmentation of the environment might allow RL agents to better approximate human and rat behavior (see Balaguer et al.<sup>110</sup>). Furthermore, the points where agents switch between different options may be able to predict where rats and humans would pause in the maze.<sup>73</sup> More broadly, new approaches to RL<sup>111</sup> and deep learning methods may provide new ways to examine navigation<sup>41,112</sup> as well as integrating our approach with biologically inspired network models that seek to explain neural dynamics during navigation.<sup>113,114</sup>

### Exploring the neural substrates of a predictive map

Recent neuroimaging in humans has shown that activity in hippocampal and connected regions tracks the modeled parameters from a SR.<sup>63,64,66,68,78</sup> Convergent evidence in rodents suggests that the place-cell activity in the dorsal cornu Ammonis 1 (CA1) of rodents may operate as a SR.<sup>67,68,71,115,116</sup> Our protocol would allow for evidence from both rodent and human data to be integrated within a single framework to consider how patterns in the data may interrelate across species and in relation to the parameters from RL-modeled agents. Evidence from other recent approaches shows the utility of such an approach.<sup>30–32</sup> Our recent analysis of CA1 place-cell activity found little evidence for changes in the place field maps when the state space changed due to blocked doorways in a 4-room maze.<sup>17</sup> However, it appears the changes in layout are evident during hippocampal replay events, where paths activated follow the new layout, perhaps consistent with MB-RL search patterns.<sup>80</sup> One consideration for future research will be to explore changes in neural activity linked to particular strategies that might occur over trials or even within a route. For example, one might predict a shift to a more striatally mediated strategy linked to MF RL, if the number of trials for a configuration was increased.<sup>51,57</sup> Shifts between the engagement of different structures to guide control may also occur alongside shifts within structures.<sup>51,81</sup> For example, the hippocampus might be involved in simulating paths via replay to guide behavior in highly dynamic environments but shift to a more cached expression of the stored hippocampal map once the possible paths have been repeatedly experienced.

Recent work modeling multi-scale SR agents<sup>117</sup> has shown patterns similar to the goal-distance-tuned activity of CA1 cells in navigating bats.<sup>118</sup> Might such patterns emerge in our task? An important step in better understanding the neural systems for navigation would be to examine the impact of temporally targeted inactivation of the hippocampal regions, as well as the prefrontal cortex, which is thought to support route planning.<sup>38</sup> Such an approach would provide more causal evidence for the role of brain structures in supporting our task. More broadly, the task

we have developed could be adapted for study with a range of other species that have been examined in isolation: ants, bees, *Drosophila*, bats, birds, and other primates. Integrating across invertebrate and vertebrate species may further our understanding of the common mechanisms for goal-directed behavior and adaptations that occurred through evolution.

### Conclusions

In summary, we found that rats and humans both display behavior most similar to a SR RL agent, with humans also showing some behavior matching MB planning. Future work exploring single-unit recording or disruption to neural activity may be useful in revealing how distance to the goal may be coded, as past studies have failed to dissociate path and Euclidean distance. Moreover, it will be useful to examine how neural activity in humans and rodents relates to the parameters from RL agents, with behavior adjusted to match the humans and rats. More broadly, the approach provided here could be adapted to compare behavior across a range of species and different RL models to help understand the broad spectrum of navigation behaviors shown by the diverse species on our planet.

### STAR★METHODS

Detailed methods are provided in the online version of this paper and include the following:

- **KEY RESOURCES TABLE**
- **RESOURCE AVAILABILITY**
  - Lead contact
  - Materials availability
  - Data and code availability
- **EXPERIMENTAL MODEL AND SUBJECT DETAILS**
- **METHOD DETAILS**
  - General methods
  - Rodent methods
  - Human methods
  - Reinforcement learner simulations
- **QUANTIFICATION AND STATISTICAL ANALYSIS**

### SUPPLEMENTAL INFORMATION

Supplemental information can be found online at <https://doi.org/10.1016/j.cub.2022.06.090>.

### ACKNOWLEDGMENTS

We would like to thank Célia Lacaux and Charles Middleton for their help in building the maze. W.d.C. was funded by an EPSRC CASE studentship with Deepmind Ltd. N.N. and H.J.S. received support from the European Union's Horizon 2020 Framework Programme for Research under Marie Skłodowska-Curie ITN (EU-M-GATE 765549). R.G. and É.D. were funded by a Wellcome Senior Investigator Award awarded to Kate J. Jeffery (103896/Z/14/Z). W.d.C., J.M.L., and C.B. are funded by a Wellcome Senior Research Fellowship awarded to C.B. (212281/Z/18/Z). H.J.S. received funding from Deepmind Ltd.

### AUTHOR CONTRIBUTIONS

Conceptualization, W.d.C. and H.J.S.; methodology, W.d.C., F.Z., S.R., D.B., R.G., É.D., C.B., and H.J.S.; formal analysis, W.d.C.; investigation, W.d.C., N.N., E.-M.G., C.G., J.M.L., L.F., and C.N.; writing—original draft, W.d.C.

and H.J.S.; writing—review & editing, W.d.C., N.N., C.N., J.M.L., D.B., R.G., É.D., C.B., and H.J.S.; visualization, W.d.C., F.Z., and H.J.S.; supervision, C.B. and H.J.S.

### DECLARATION OF INTERESTS

The authors declare no competing interests.

Received: March 15, 2022

Revised: May 19, 2022

Accepted: June 29, 2022

Published: July 20, 2022

### REFERENCES

1. Ekstrom, A.D., Spiers, H.J., Bohbot, V.D., and Rosenbaum, R.S. (2018). *Human Spatial Navigation* (Princeton University Press).
2. Gallistel, C.R. (1990). *The Organization of Learning* (The MIT Press).
3. Behrens, T.E.J., Muller, T.H., Whittington, J.C.R., Mark, S., Baram, A.B., Stachenfeld, K.L., and Kurth-Nelson, Z. (2018). What is a cognitive map? Organizing knowledge for flexible behavior. *Neuron* 100, 490–509.
4. Epstein, R.A., Patai, E.Z., Julian, J.B., and Spiers, H.J. (2017). The cognitive map in humans: spatial navigation and beyond. *Nat. Neurosci.* 20, 1504–1513.
5. Tolman, E.C. (1948). Cognitive maps in rats and men. *Psychol. Rev.* 55, 189–208.
6. Tolman, E.C., and Honzik, C.H. (1930). *Introduction and Removal of Reward, and Maze Performance in Rats* (University of California Press).
7. Alvernhe, A., Van Cauter, T.V., Save, E., and Poucet, B. (2008). Different CA1 and CA3 representations of novel routes in a shortcut situation. *J. Neurosci.* 28, 7324–7333.
8. Brown, T.I., Gagnon, S.A., and Wagner, A.D. (2020). Stress disrupts human hippocampal-prefrontal function during prospective spatial navigation and hinders flexible behavior. *Curr. Biol.* 30, 1821–1833.e8.
9. Grieves, R.M., and Dudchenko, P.A. (2013). Cognitive maps and spatial inference in animals: rats fail to take a novel shortcut, but can take a previously experienced one. *Learn. Motiv.* 44, 81–92.
10. Howard, L.R., Javadi, A.H., Yu, Y., Mill, R.D., Morrison, L.C., Knight, R., Loftus, M.M., Staskute, L., and Spiers, H.J. (2014). The hippocampus and entorhinal cortex encode the path and euclidean distances to goals during navigation. *Curr. Biol.* 24, 1331–1340.
11. Javadi, A.H., Emo, B., Howard, L.R., Zisch, F.E., Yu, Y., Knight, R., Pinelo Silva, J., and Spiers, H.J. (2017). Hippocampal and prefrontal processing of network topology to simulate the future. *Nat. Commun.* 8, 14652.
12. Javadi, A.H., Patai, E.Z., Marin-Garcia, E., Margois, A., Tan, H.-R.M., Kumaran, D., Nardini, M., Penny, W., Duzel, E., Dayan, P., et al. (2019). Backtracking during navigation is correlated with enhanced anterior cingulate activity and suppression of alpha oscillations and the 'default-mode' network. *Proc. Biol. Sci.* 286, 20191016.
13. Patai, E.Z., Javadi, A.H., Ozubko, J.D., O'Callaghan, A., Ji, S., Robin, J., Grady, C., Winocur, G., Rosenbaum, R.S., Moscovitch, M., et al. (2019). Hippocampal and retrosplenial goal distance coding after long-term consolidation of a real-world environment. *Cereb. Cortex* 29, 2748–2758.
14. Shamash, P., Olesen, S.F., Iordanidou, P., Campagner, D., Banerjee, N., and Branco, T. (2021). Mice learn multi-step routes by memorizing sub-goal locations. *Nat. Neurosci.* 24, 1270–1279.
15. Tolman, E.C., Ritchie, B.F., and Kalish, D. (1946). Studies in spatial learning. I. Orientation and the short-cut. *J. Exp. Psychol.* 36, 13–24.
16. Xu, J., Evensmoen, H.R., Lehn, H., Pintzka, C.W., and Häberg, A.K. (2010). Persistent posterior and transient anterior medial temporal lobe activity during navigation. *NeuroImage* 52, 1654–1666.
17. Duvelle, É., Grieves, R.M., Liu, A., Jedidi-Ayoub, S., Holeniewska, J., Harris, A., Nyberg, N., Donnarumma, F., Lefort, J.M., Jeffery, K.J.,

- et al. (2021). Hippocampal place cells encode global location but not connectivity in a complex space. *Curr. Biol.* *31*, 1221–1233.e9.
18. Spiers, H.J., and Gilbert, S.J. (2015). Solving the detour problem in navigation: a model of prefrontal and hippocampal interactions. *Front. Hum. Neurosci.* *9*, 125.
  19. Gentry, G., Brown, W.L., and Kaplan, S.J. (1947). An experimental analysis of the spatial location hypothesis in learning. *J. Comp. Physiol. Psychol.* *40*, 309–322.
  20. Foo, P., Warren, W.H., Duchon, A., and Tarr, M.J. (2005). Do humans integrate routes into a cognitive map? Map- versus landmark-based navigation of novel shortcuts. *J. Exp. Psychol. Learn. Mem. Cogn.* *31*, 195–215.
  21. Marchette, S.A., Bakker, A., and Shelton, A.L. (2011). Cognitive mappers to creatures of habit: differential engagement of place and response learning mechanisms predicts human navigational behavior. *J. Neurosci.* *31*, 15264–15268.
  22. Ekstrom, A.D., and Ranganath, C. (2018). Space, time, and episodic memory: the hippocampus is all over the cognitive map. *Hippocampus* *28*, 680–687.
  23. Gahnstrom, C.J., and Spiers, H.J. (2020). Striatal and hippocampal contributions to flexible navigation in rats and humans. *Brain Neurosci. Adv.* *4*, 2398212820979772.
  24. Nyberg, N., Duvelle, É., Barry, C., and Spiers, H.J. (2022). Spatial goal coding in the hippocampal formation. *Neuron* *110*, 394–422.
  25. O’Keefe, J., and Nadel, L. (1978). *The Hippocampus as a Cognitive Map* (Clarendon Press).
  26. Spiers, H.J., and Barry, C. (2015). Neural systems supporting navigation. *Curr. Opin. Behav. Sci.* *1*, 47–55.
  27. Ekstrom, A.D., Kahana, M.J., Caplan, J.B., Fields, T.A., Isham, E.A., Newman, E.L., and Fried, I. (2003). Cellular networks underlying human spatial navigation. *Nature* *425*, 184–188.
  28. Grieves, R.M., and Jeffery, K.J. (2017). The representation of space in the brain. *Behav. Processes* *135*, 113–131.
  29. Poulter, S., Hartley, T., and Lever, C. (2018). The neurobiology of mammalian navigation. *Curr. Biol.* *28*, R1023–R1042.
  30. Barron, H.C., Reeve, H.M., Koolschijn, R.S., Perestenko, P.V., Shpektor, A., Nili, H., Rothaermel, R., Campo-Urriza, N., O’Reilly, J.X., Bannerman, D.M., et al. (2020). Neuronal computation underlying inferential reasoning in humans and mice. *Cell* *183*, 228–243.e21.
  31. Barron, H.C., Mars, R.B., Dupret, D., Lerch, J.P., and Sampaio-Baptista, C. (2021). Cross-species neuroscience: closing the explanatory gap. *Philos. Trans. R. Soc. Lond. B Biol. Sci.* *376*, 20190633.
  32. Samanta, A., van Rongen, L.S., Rossato, J.I., Jacobse, J., Schoenfeld, R., and Genzel, L. (2021). Sleep leads to brain-wide neural changes independent of allocentric and egocentric spatial training in humans and rats. *Cereb. Cortex* *31*, 4970–4985.
  33. Coughlan, G., Laczó, J., Hort, J., Minihane, A.M., and Hornberger, M. (2018). Spatial navigation deficits—overlooked cognitive marker for pre-clinical Alzheimer disease? *Nat. Rev. Neurol.* *14*, 496–506.
  34. Coughlan, G., Coutrot, A., Khondoker, M., Minihane, A.M., Spiers, H., and Hornberger, M. (2019). Toward personalized cognitive diagnostics of at-genetic-risk Alzheimer’s disease. *Proc. Natl. Acad. Sci. USA* *116*, 9285–9292.
  35. Laczó, J., Andel, R., Vyhnaek, M., Vlcek, K., Magerova, H., Varjassyova, A., Nedelska, Z., Gazova, I., Bojar, M., Sheardova, K., et al. (2012). From Morris water maze to computer tests in the prediction of Alzheimer’s disease. *Neurodegener. Dis.* *10*, 153–157.
  36. McGann, J.P. (2017). Poor human olfaction is a 19th-century myth. *Science* *356*, eaam7263.
  37. Wallace, D.J., Greenberg, D.S., Sawinski, J., Rulla, S., Notaro, G., and Kerr, J.N.D. (2013). Rats maintain an overhead binocular field at the expense of constant fusion. *Nature* *498*, 65–69.
  38. Patai, E.Z., and Spiers, H.J. (2021). The versatile Wayfinder: prefrontal contributions to spatial navigation. *Trends Cogn. Sci.* *25*, 520–533.
  39. Uylings, H.B.M., Groenewegen, H.J., and Kolb, B. (2003). Do Rats Have a Prefrontal Cortex? (Elsevier).
  40. Andersen, P., Morris, R., Amaral, D., Bliss, T., and O’Keefe, J. (2006). *The Hippocampus Book* (Oxford University Press).
  41. Banino, A., Barry, C., Uria, B., Blundell, C., Lillicrap, T., Mirowski, P., Pritzel, A., Chadwick, M.J., Degris, T., Modayil, J., et al. (2018). Vector-based navigation using grid-like representations in artificial agents. *Nature* *557*, 429–433.
  42. Bermudez-Contreras, E., Clark, B.J., and Wilber, A. (2020). The neuroscience of spatial navigation and the relationship to artificial intelligence. *Front. Comput. Neurosci.* *14*, 63.
  43. Botvinick, M., Wang, J.X., Dabney, W., Miller, K.J., and Kurth-Nelson, Z. (2020). *Deep Reinforcement Learning and Its Neuroscientific Implications* (Cell Press).
  44. Dayan, P., and Daw, N.D. (2008). *Decision Theory, Reinforcement Learning, and the Brain* (Springer).
  45. Momennejad, I. (2020). *Learning Structures: Predictive Representations, Replay, and Generalization* (Elsevier Ltd).
  46. Simon, D.A., and Daw, N.D. (2011). Neural correlates of forward planning in a spatial decision task in humans. *J. Neurosci.* *31*, 5526–5539.
  47. Mnih, V., Kavukcuoglu, K., Silver, D., Rusu, A.A., Veness, J., Bellemare, M.G., Graves, A., Riedmiller, M., Fidjeland, A.K., Ostrovski, G., et al. (2015). Human-level control through deep reinforcement learning. *Nature* *518*, 529–533.
  48. Silver, D., Huang, A., Maddison, C.J., Guez, A., Sifre, L., van den Driessche, G., Schrittwieser, J., Antonoglou, I., Panneershelvam, V., Lanctot, M., et al. (2016). Mastering the game of Go with deep neural networks and tree search. *Nature* *529*, 484–489.
  49. Silver, D., Schrittwieser, J., Simonyan, K., Antonoglou, I., Huang, A., Guez, A., Hubert, T., Baker, L., Lai, M., Bolton, A., et al. (2017). Mastering the game of Go without human knowledge. *Nature* *550*, 354–359.
  50. Anggraini, D., Glasauer, S., and Wunderlich, K. (2018). Neural signatures of reinforcement learning correlate with strategy adoption during spatial navigation. *Sci. Rep.* *8*, 10110.
  51. Geerts, J.P., Chersi, F., Stachenfeld, K.L., and Burgess, N. (2020). A general model of hippocampal and dorsal striatal learning and decision making. *Proc. Natl. Acad. Sci. USA* *117*, 31427–31437.
  52. Voudouris, K., Crosby, M., Beyret, B., Hernández-Orallo, J., Shanahan, M., Halina, M., and Cheke, L.G. (2022). Direct human-AI comparison in the animal-AI environment. *Front. Psychol.* *13*, 711821.
  53. Zhu, S.L., Lakshminarasimhan, K.J., Arfaei, N., and Angelaki, D.E. (2021). Eye movements reveal spatiotemporal dynamics of active sensing and planning in navigation. *Elife* *11*, e73097.
  54. Sutton, R.S., and Barto, A.G. (2018). *Reinforcement Learning: an Introduction, Second Edition* (MIT Press).
  55. Sutton, R.S. (1988). Learning to predict by the methods of temporal differences. *Mach. Learn.* *3*, 9–44.
  56. Watkins, C.J.C.H., and Dayan, P. (1992). Q-learning. *Mach. Learn.* *8*, 279–292.
  57. Dolan, R.J., and Dayan, P. (2013). Goals and habits in the brain. *Neuron* *80*, 312–325.
  58. Lee, J.J., and Keramati, M. (2017). Flexibility to contingency changes distinguishes habitual and goal-directed strategies in humans. *PLoS Comput. Biol.* *13*, e1005753.
  59. Dayan, P. (1993). Improving generalization for temporal difference learning: the successor representation. *Neural Comput.* *5*, 613–624.
  60. Gershman, S.J. (2018). The successor representation: its computational logic and neural substrates. *J. Neurosci.* *38*, 7193–7200.
  61. Russek, E.M., Momennejad, I., Botvinick, M.M., Gershman, S.J., and Daw, N.D. (2017). Predictive representations can link model-based

- reinforcement learning to model-free mechanisms. *PLoS Comput. Biol.* **13**, e1005768.
62. Bellmund, J.L.S., de Cothi, W., Ruiter, T.A., Nau, M., Barry, C., and Doeller, C.F. (2019). Deforming the metric of cognitive maps distorts memory. *Nat. Hum. Behav.* **4**, 177–188.
63. Brunec, I.K., and Momennejad, I. (2019). Predictive representations in hippocampal and prefrontal hierarchies. Preprint at bioRxiv. <https://doi.org/10.1101/786434>.
64. Garvert, M.M., Dolan, R.J., and Behrens, T.E. (2017). A map of abstract relational knowledge in the human hippocampal–entorhinal cortex. *eLife* **6**, 1–20.
65. Momennejad, I., Russek, E.M., Cheong, J.H., Botvinick, M.M., Daw, N.D., and Gershman, S.J. (2017). The successor representation in human reinforcement learning. *Nat. Hum. Behav.* **1**, 680–692.
66. Russek, E.M., Momennejad, I., Botvinick, M.M., Gershman, S.J., and Daw, N.D. (2021). Neural evidence for the successor representation in choice evaluation. Preprint at bioRxiv. <https://doi.org/10.1101/2021.08.29.458114>.
67. de Cothi, W., and Barry, C. (2020). Neurobiological successor features for spatial navigation. *Hippocampus* **30**, 1347–1355.
68. Stachenfeld, K.L., Botvinick, M.M., and Gershman, S.J. (2017). The hippocampus as a predictive map. *Nat. Neurosci.* **20**, 1643–1653.
69. Daw, N.D., Gershman, S.J., Seymour, B., Dayan, P., and Dolan, R.J. (2011). Model-based influences on humans' choices and striatal prediction errors. *Neuron* **69**, 1204–1215.
70. Miller, K.J., Botvinick, M.M., and Brody, C.D. (2017). Dorsal hippocampus contributes to model-based planning. *Nat. Neurosci.* **20**, 1269–1276.
71. Sosa, M., and Giocomo, L.M. (2021). Navigating for reward. *Nat. Rev. Neurosci.* **22**, 472–487.
72. George, T.M., de Cothi, W., Stachenfeld, K., and Barry, C. (2022). Rapid Learning of predictive maps with STDP and theta phase precession. Preprint at bioRxiv. <https://doi.org/10.1101/2022.04.20.488882>.
73. Redish, A.D. (2016). Vicarious trial and error. *Nat. Rev. Neurosci.* **17**, 147–159.
74. Vikbladh, O.M., Meager, M.R., King, J., Blackmon, K., Devinsky, O., Shohamy, D., Burgess, N., and Daw, N.D. (2019). Hippocampal contributions to model-based planning and spatial memory. *Neuron* **102**, 683–693.e4.
75. Wunderlich, K., Smittenaar, P., and Dolan, R.J. (2012). Dopamine enhances model-based over model-free choice behavior. *Neuron* **75**, 418–424.
76. Baram, A.B., Muller, T.H., Whittington, J.C.R., and Behrens, T.E.J. (2018). Intuitive planning: global navigation through cognitive maps based on grid-like codes. bioRxiv. 421461.
77. Mattar, M.G., and Daw, N.D. (2018). Prioritized memory access explains planning and hippocampal replay. *Nat. Neurosci.* **21**, 1609–1617.
78. Momennejad, I., Otto, A.R., Daw, N.D., and Norman, K.A. (2018). Offline replay supports planning in human reinforcement learning. *eLife* **7**, 1–25.
79. Pfeiffer, B.E., and Foster, D.J. (2013). Hippocampal place-cell sequences depict future paths to remembered goals. *Nature* **497**, 74–79.
80. Widloski, J., and Foster, D.J. (2022). Flexible rerouting of hippocampal replay sequences around changing barriers in the absence of global place field remapping. *Neuron* **110**, 1547–1558.e8.
81. Daw, N.D., Niv, Y., and Dayan, P. (2005). Uncertainty-based competition between prefrontal and dorsolateral striatal systems for behavioral control. *Nat. Neurosci.* **8**, 1704–1711.
82. Alvernhe, A., Save, E., and Poucet, B. (2011). Local remapping of place cell firing in the Tolman detour task. *Eur. J. Neurosci.* **33**, 1696–1705.
83. Rosenberg, M., Zhang, T., Perona, P., and Meister, M. (2021). Mice in a labyrinth show rapid learning, sudden insight, and efficient exploration. *eLife* **10**, e66175.
84. Zisch, F.E., Newton, C., Coutrot, A., Murcia, M., Motala, A., Greaves, J., de Cothi, W. de, Steed, A., Tyler, N., Gage, S.A., et al. (2022). Comparable human spatial memory distortions in physical, desktop virtual and immersive virtual environments. Preprint at bioRxiv. <https://doi.org/10.1101/2022.01.11.475791>.
85. Heffner, R.S., and Heffner, H.E. (1992). Visual factors in sound localization in mammals. *J. Comp. Neurol.* **317**, 219–232.
86. Small, W.S. (1901). Experimental study of the mental processes of the rat. *II. Am. J. Psychol.* **12**, 206–239.
87. Wiener, J.M., Büchner, S.J., and Hölscher, C. (2009). Taxonomy of human Wayfinding tasks: A knowledge-based approach. *Spat. Cogn. Comput.* **9**, 152–165.
88. Morris, R. (1984). Developments of a water-maze procedure for studying spatial learning in the rat. *J. Neurosci. Methods* **11**, 47–60.
89. Tessereau, C., O'Dea, R., Coombes, S., and Bast, T. (2021). Reinforcement learning approaches to hippocampus-dependent flexible spatial navigation. *Brain Neurosci. Adv.* **5**. 2398212820975634.
90. Wood, R.A., Bauza, M., Krupic, J., Burton, S., Delekate, A., Chan, D., and O'Keefe, J. (2018). The honeycomb maze provides a novel test to study hippocampal-dependent spatial navigation. *Nature* **554**, 102–105.
91. Mobbs, D., Wise, T., Suthana, N., Guzmán, N., Kriegeskorte, N., and Leibo, J.Z. (2021). Promises and challenges of human computational ethology. *Neuron* **109**, 2224–2238.
92. Alonso, A., Bokeria, L., Meij, J. van der, Samanta, A., Eichler, R., Spooner, P., Lobato, I.N., and Genzel, L. (2020). The HexMaze: a previous knowledge and schema task for mice. Preprint at bioRxiv. <https://doi.org/10.1101/441048>.
93. Alvernhe, A., Sargolini, F., and Poucet, B. (2012). Rats build and update topological representations through exploration. *Anim. Cogn.* **15**, 359–368.
94. Poucet, B., and Herrmann, T. (2001). Exploratory patterns of rats on a complex maze provide evidence for topological coding. *Behav. Processes* **53**, 155–162.
95. Uster, H.J., Bättig, K., and Nägeli, H.H. (1976). Effects of maze geometry and experience on exploratory behavior in the rat. *Anim. Learn. Behav.* **4**, 84–88.
96. Vallianatou, C.A., Alonso, A., Aleman, A.Z., Genzel, L., and Stella, F. (2021). Learning-induced shifts in mice navigational strategies are unveiled by a minimal behavioral model of spatial exploration. *eNeuro* **8**. ENEURO.0553-20.2021.
97. Ellard, C.G., and Eller, M.C. (2009). Spatial cognition in the gerbil: computing optimal escape routes from visual threats. *Anim. Cogn.* **12**, 333–345.
98. Dollé, L., Chavarriga, R., Guillot, A., and Khamassi, M. (2018). Interactions of spatial strategies producing generalization gradient and blocking: A computational approach. *PLOS Comput. Biol.* **14**, e1006092.
99. Javadi, A.H., Patai, E.Z., Marin-Garcia, E., Margolis, A., Tan, H.-R.M., Kumaran, D., Nardini, M., Penny, W., Duzel, E., Dayan, P., et al. (2019). Prefrontal dynamics associated with efficient detours and shortcuts: A combined functional magnetic resonance imaging and Magnetoencephalography study. *J. Cogn. Neurosci.* **31**, 1227–1247.
100. Spiers, H.J., and Maguire, E.A. (2006). Thoughts, behavior, and brain dynamics during navigation in the real world. *NeuroImage* **31**, 1826–1840.
101. Meyer, A.F., O'Keefe, J., and Poort, J. (2020). Two distinct types of eye-head coupling in freely moving mice. *Curr. Biol.* **30**, 2116–2130.e6.
102. Kryven, M., Yu, S., Kleiman-Weiner, M., and Tenenbaum, J. (2021). Adventures of human planners in maze search task. Preprint at PsyarXiv. <https://doi.org/10.31234/osf.io/r5hd4>.
103. Sutton, R.S. (1990). Integrated architectures for learning, planning, and reacting based on approximating dynamic programming. In *Machine Learning Proceedings (Elsevier)*, pp. 216–224.
104. Liu, Y., Dolan, R.J., Kurth-Nelson, Z., and Behrens, T.E.J. (2019). Human replay spontaneously reorganizes experience. *Cell* **178**, 640–652.e14.

105. Liu, Y., Mattar, M.G., Behrens, T.E.J., Daw, N.D., and Dolan, R.J. (2021). Experience replay is associated with efficient nonlocal learning. *Science* *372*, eabf1357.
106. Still, S., and Precup, D. (2012). An information-theoretic approach to curiosity-driven reinforcement learning. *Theory Biosci.* *131*, 139–148.
107. Geerts, J., Stachenfeld, K., and Burgess, N. (2019). Probabilistic successor representations with Kalman temporal differences. In *Conference on Cognitive Computational Neuroscience*.
108. Gershman, S.J. (2015). A unifying probabilistic view of associative learning. *PLoS Comput. Biol.* *11*, e1004567.
109. Stolle, M., and Precup, D. (2002). Learning options in reinforcement learning. In *Abstraction, Reformulation, and Approximation Lecture Notes in Computer Science*, S. Koenig, and R.C. Holte, eds. (Springer), pp. 212–223.
110. Balaguer, J., Spiers, H., Hassabis, D., and Summerfield, C. (2016). Neural mechanisms of hierarchical planning in a virtual subway network. *Neuron* *90*, 893–903.
111. Piray, P., and Daw, N.D. (2021). Linear reinforcement learning in planning, grid fields, and cognitive control. *Nat. Commun.* *12*, 4942.
112. Frey, M., Tanni, S., Perrodin, C., O’Leary, A., Nau, M., Kelly, J., Banino, A., Bendor, D., Lefort, J., Doeller, C.F., et al. (2021). Interpreting wide-band neural activity using convolutional neural networks. *eLife* *10*, e66551.
113. Erdem, U.M., and Hasselmo, M. (2012). A goal-directed spatial navigation model using forward trajectory planning based on grid cells. *Eur. J. Neurosci.* *35*, 916–931.
114. Kubie, J.L., and Fenton, A.A. (2009). Heading-vector navigation based on head-direction cells and path integration. *Hippocampus* *19*, 456–479.
115. Mehta, M.R., Quirk, M.C., and Wilson, M.A. (2000). Experience-dependent asymmetric shape of hippocampal receptive fields. *Neuron* *25*, 707–715.
116. Mehta, M.R., Barnes, C.A., and McNaughton, B.L. (1997). Experience-dependent, asymmetric expansion of hippocampal place fields. *Proc. Natl. Acad. Sci. USA* *94*, 8918–8921.
117. Momennejad, I., and Howard, M.W. (2018). Predicting the future with multi-scale successor representations. Preprint at bioRxiv. <https://doi.org/10.1101/449470>.
118. Sarel, A., Finkelstein, A., Las, L., and Ulanovsky, N. (2017). Vectorial representation of spatial goals in the hippocampus of bats. *Science* *355*, 176–180.
119. Clemens, L.E., Jansson, E.K.H., Portal, E., Riess, O., and Nguyen, H.P. (2014). A behavioral comparison of the common laboratory rat strains Lister Hooded, Lewis, Fischer 344 and Wistar in an automated homecage system. *Genes Brain Behav. (Fischer)* *13*, 305–321.
120. Hart, P.E., Nilsson, N.J., and Raphael, B. (1968). A formal basis for the heuristic determination of minimum cost paths. *IEEE Trans. Syst. Sci. Cybern.* *4*, 100–107.
121. Gershman, S.J., Moore, C.D., Todd, M.T., Norman, K.A., and Sederberg, P.B. (2012). The successor representation and temporal context. *Neural Comput.* *24*, 1553–1568.

## STAR★METHODS

### KEY RESOURCES TABLE

REAGENT or RESOURCE	SOURCE	IDENTIFIER
Deposited data		
Data and Code	Zenodo	<a href="https://doi.org/10.5281/zenodo.6734981">https://doi.org/10.5281/zenodo.6734981</a>

### RESOURCE AVAILABILITY

#### Lead contact

Further information and requests for resources should be directed to and will be fulfilled by the lead contact William de Cothi ([w.decothi@ucl.ac.uk](mailto:w.decothi@ucl.ac.uk)).

#### Materials availability

This study did not generate any unique reagents.

#### Data and code availability

All data and code have been deposited at zenodo and are publicly available as of the date of publication. DOIs are listed in the [key resources table](#).

### EXPERIMENTAL MODEL AND SUBJECT DETAILS

Nine adult male Lister Hooded rats were handled daily (at start of training: 10–20 weeks old, 350–400 g) and housed communally in groups of three. All rats were subjected to a reverse light-dark cycle (11:11 light:dark, with 1 hour x2 simulated dawn/dusk) and were on food-restriction sufficient to maintain 90% of free-feeding weight, with ad libitum access to water. The free-feeding weight was continuously adjusted according to a calculated growth curve for Lister Hooded Rats.<sup>119</sup> Six rats were naive, while three rats had previously been trained for 2–3 weeks in a shortcut navigation task for a different maze setup. The procedures were conducted according to UCL ethical guidelines and licensed by the UK Home Office subject to the restrictions and provisions contained in the Animals Scientific Procedures Act of 1986.

For the human version of the task, 18 healthy participants (9 female; aged =  $24.6 \pm 5.9$ , mean  $\pm$  sd) were recruited from the UCL Psychology Subject Pool and trained to navigate to an unmarked goal in a virtual arena of approximately the same relative proportion as for the rats. All participants gave written consent to participate in the study in accordance with the UCL Research Ethics Committee.

### METHOD DETAILS

#### General methods

Navigation was tested in a large square environment with a fixed hidden goal location and a prominent directional black wall cue in one direction (Figure 1; Videos S1 and S2). The maze was divided in a 10x10 grid of moveable sections that could either be removed, leaving impassable gaps to force detour taking, or added, creating shortcuts. During training, all maze modules were present. Rats, humans and RL agents were trained to reach the goal within a 45s time limit (Figure 1A). During the testing phase of the experiment, maze modules were removed to block the direct route to the goal (Figure 1B). Humans (n=18), rats (n=9) and agents were tested on the same sequence of 25 maze configurations each with 10 trials in which a set of defined starting locations were selected to optimally probe navigation (Figure 1C). These maze configurations were generated from a pilot testing with 9 rats and the configuration sequence chosen maximised the differences in the layouts between trials. The starting positions on each maze configuration gradually increased in the required tortuosity (path distance / Euclidean distance) of the shortest path to the goal to test complex trajectories whilst keeping the rodents motivated.

Upon reaching the goal module, rats and humans had to wait 5s to receive their reward. Human participants were rewarded with a financial bonus and rats received chocolate milk delivered in a well (Figure S1). In order to better match the visual acuity and depth perception between rodents and humans,<sup>85</sup> a thick virtual fog lined the floor of the maze enabling them to only see adjacent maze modules and the distal black wall cue (Figure S2; Video S2). Modules were made visually indistinct to avoid humans counting them when traversing the space. Human participants were informed that reward was hidden in the environment and that their task was to maximise their financial return as quickly and efficiently as possible. The human and rat trajectories were discretised into the underlying 10x10 modular grid (Figures 2A and 2B) in order to facilitate comparison between each other and the RL agents.



In all versions of the experiment, the environment (raised off the floor) consisted of a 10x10 grid of maze modules. These modules could be removed from the grid in order to form impassable barriers in the environment. One of the modules was rewarded and thus was the location of the goal in the maze. Navigation was facilitated by a single distal cue consisting of a black curtain that spanned the majority of one side of the maze. The goal was kept in the same position with respect to this distal cue throughout all versions of the task. All participants, rats and learning agents were initially trained to navigate to the goal module on the open maze, without any maze modules removed. Once trained, they were all put through the same sequence of 25 maze configurations, with the same sequence of starting locations on each configuration.

### Rodent methods

All procedures were conducted during the animals' dark period. The experiment was carried out in a custom-made modular 2x2m square maze composed of 100 identical square platform tiles elevated 50cm above the ground (Figure S1). The maze was constructed from Medium Density Fibrewood, with the platforms painted in grey. Each platform contained a plastic well (32mm diameter) at its centre, which could be attached to a polymeric tubing system installed beneath the maze. This tubing allowed the experimenter to reward the rat at the goal module filling the well with chocolate milk (0.1 ml). Importantly, all modules in the rodent maze were identical in appearance and construction with chocolate milk rubbed into the well of non-goal modules to lower reliance on olfactory navigational cues. The maze was surrounded on all sides by a white curtain, with a black sheet overlaid on one side to provide a single extra-maze cue. To ensure that no other cue could be used by the animal (uncontrolled room cues, olfactory traces on the maze) the black sheet was rotated 90° clockwise between sessions. The goal module was always in the same position with respect to this cue. Moreover, the experimenter stayed next to the maze inside the curtained area throughout all sessions, his positions relative to the goal were randomised.

#### Familiarisation

During the first day, the rats received a small amount (0.1ml per rat) of chocolate milk in the home cage to decrease neophobia in the maze. For the subsequent two days, each rat underwent two 15 minute maze familiarisation sessions, in which the rat was placed at the centre of the maze and would forage for pieces of chocolate cereal (Weetos) scattered throughout the maze. More cereal was concentrated in the centre to encourage the animal to be comfortable in the middle of the maze.

#### Training

Training consisted of two stages, rats were given 2 training sessions per day. In each training trial the rat had 45s to find the goal module.

For stage 1 of training the goal well was filled with 0.1ml of chocolate milk and the rats were initially placed on the modules adjacent to the goal, facing the goal. If the rat made two consecutive direct runs to the goal (without exploration of other parts of the maze), the next trial began one module further away from the goal. Conversely, if the rat failed two consecutive training trials, the next trial began one module closer to the goal until the rat was back at the goal-adjacent modules. On day 1, this procedure was continued until 15 min had elapsed. On the following days, the number of trials was fixed to 16. This procedure was followed every day until the rat was able to make direct runs from the far edges of the maze.

Stage 2 was similar to stage 1 but a delay in the release of chocolate milk was introduced. This delay started at 1s and was gradually increased until the rat could wait at the goal location for 5s before the chocolate milk was released. Furthermore, the rat's starting position and orientation were randomised. The number of daily trials could be increased up to 25. This procedure was followed until the rats were able to successfully navigate directly to the goal and on at least 90% of trials. The training phase took on average 24 sessions.

#### Tartarus Maze testing

Rats were run on the 25 maze configurations. For each maze configuration, rats were given 10 trials where they were placed by hand at the starting positions indicated in Figure 1. Trials were 45s long and rats were required to navigate to the goal within this time and wait for 5s in order to receive the reward (0.1ml of chocolate milk). If the rat failed to reach the goal, they received no reward and were placed by hand at the next starting location. The rats would usually complete 3 configurations per day. At the beginning of each day, rats were given a brief reminder session that consisted of 5 trials from phase 2 of the training phase.

### Human methods

Participants were reimbursed for their time as well as a bonus of up to £25 for good performance in the testing phase. Participants experienced the virtual environment via a HTC Vive virtual reality headset whilst sat on a swivel chair. They were able to adjust movement speed using the HTC Vive controller and movement direction was controlled by the participant's orientation on the chair. Upon successful navigation to the goal module, participants were informed of their financial reward along with the presence of a revolving gold star (Figure S2) at the goal location. In accordance with the rodent experiment, navigation was aided by the presence of a black distal cue that took up the majority of one of the walls. Goal location, maze configurations and starting positions were all defined with respect to this distal cue and were identical to the rodent experiment. Importantly, a fog lined the floor (Figure S2; Video S2) of the maze to prevent the participants from understanding what maze modules were missing until they were at adjacent locations. This also provided a better match to visual information available to the rats - which are known to have less visual acuity and binocular depth perception.<sup>85</sup> Seamless textures were applied to the floor and walls of the virtual environment, and these were rotated every 10 trials to prevent them from being used as extraneous cues for navigation.

The experiment took place over four sessions on four consecutive days. The majority of the first session was usually spent training the participants to navigate to the goal module. To accelerate this learning process, the participants were initially able to see a revolving gold star in the goal location. As they progressed through the training session the star became increasingly transparent until invisible, with the star only appearing again upon successful navigation to the goal module. Along with the decreasing visibility of the goal, the participants' starting positions were moved progressively further from the goal in a similar manner to the rat training phase. All training and testing trials were 45s in length. Training was terminated when the participants were able to navigate to the hidden goal on at least 80% of trials after being randomly placed at the far edges of the environment. Mean time to complete this training was  $41 \pm 21$  minutes. In order to make the participants' experience similar to that of the rodents, they were not given any explicit information about the nature of the task - only that financial reward was hidden in the environment in the form of a gold star and their task was to maximise their financial return as quickly and efficiently as possible.

The testing took place over the remaining sessions and on average lasted  $125 \pm 25$  minutes, with participants encouraged to take short breaks every 10-20 trials to reduce virtual reality sickness. At the beginning of each testing session, participants completed a short reminder task, which consisted of 5 trials from the end of the training phase.

### Reinforcement learner simulations

Reinforcement learning seeks to address how an agent should choose actions in order to maximise its expected accumulated reward  $R$  yielded from future states  $\mathbf{s}_t$ , which is known as the value function  $V$ :

$$V(\mathbf{s}) = \mathbb{E} \left[ \sum_{t=0}^{\infty} \gamma^t R(\mathbf{s}_t) | \mathbf{s}_0 = \mathbf{s} \right]$$

The parameter  $\gamma$  is a discount factor that determines the timescale of how motivating future rewards are, such that for  $\gamma < 1$  the agent exponentially discounts future rewards.<sup>54</sup>

The reinforcement learning agents were implemented in a 10x10 grid world environment, with each state in the grid world corresponding to a maze module in the human/rat versions of the task (see [Figures S1](#) and [S2](#)). Thus, unlike the humans and rats, the agents were not explicitly required to self-localise with respect to distal cues, rather they were given absolute knowledge of their current location (state) on the maze in the form of a one-hot vector (a vector with a '1' in the element corresponding to the current state, with all other elements in the vector being '0'). Upon receiving this information pertaining to its current location, the agent was able to choose actions (i.e. up, down, left, right) which transition it to adjacent states, with the ultimate aim being to choose a sequence of states leading to the goal. Crucially, the way in which an agent chooses this sequence of states is different for the model-free, model-based and successor representation algorithms - which are explained in more detail below. At the beginning of the experiment, all agents were endowed with the optimal policy on the open maze to simulate the training phase undertaken by rats and humans. They were then run consecutively on the 25 maze configurations, using the maximum likelihood parameters fit to each individual rat or human participant's data. For a given individual rat or human, agent behaviour was simulated on each maze configuration by first training the agent on all of that individual's trajectories (in the same sequential order) prior to the configuration being simulated. Agents then carried over all models/value representations learnt during their 10 trials on the maze configuration being simulated. Hence, the simulated behaviour of agents was never trained using the human/rat trajectories on the configuration being simulated, only the trajectories on all configurations prior. Each type of agent (model-free, model-based and successor representation) was simulated  $N=100$  times per rat/human, using an  $\epsilon$ -greedy policy with  $\epsilon$  linearly decaying from  $\epsilon = 0.1$  to  $\epsilon = 0.01$  across the 10 trials on a maze configuration. This means that on a new configuration the agents initially chose the greedy action 90% of the time and a random action the remaining 10% of the time (in order to manage the exploration-exploitation tradeoff), with the agents increasing the proportion of greedy actions they take by 1% on each subsequent trial. Due to the behavioural variance introduced by this policy, each algorithm was implemented 100 times for each rat/human to produce the distribution of behaviour used for the comparison with biology. In the subsequent analyses, each individual rat or human was compared to the simulated agents trained on their behaviour, using the maximum likelihood parameters fit to their behaviour.

#### Model-free agent

The model-free method uses the state-action value function  $Q$  instead of the state value function  $V$ .

$$Q(\mathbf{s}, a) = \mathbb{E} \left[ \sum_{t=0}^{\infty} \gamma^t R(\mathbf{s}_t) | \mathbf{s}_0 = \mathbf{s}, a_0 = a \right]$$

State-action values were learned using the Q-learning algorithm<sup>56</sup> combined with an eligibility trace.<sup>54</sup> The eligibility trace is a decaying trace of recently taken state-action pairs. Specifically, after taking action  $a_t$  in state  $\mathbf{s}_t$  and transitioning to state  $\mathbf{s}_{t+1}$  where it receives reward  $r_t$ , the agent will first decay its eligibility trace  $e$  - a matrix with the same dimensions as  $Q$ :

$$e \leftarrow \lambda \gamma e$$

where  $\lambda = 0.5$  is the eligibility trace decay parameter and  $\gamma$  is the discount factor of the value function in [Tables S1](#) and [S2](#). Next, the model-free agent will update its eligibility trace:

$$e(\mathbf{s}_t, a_t) \leftarrow e(\mathbf{s}_t, a_t) + 1$$

before finally updating the state-action values according to:

$$Q \leftarrow Q + \alpha \left[ r_t + \gamma \max_a Q(\mathbf{s}_{t+1}, a) - Q(\mathbf{s}_t, a_t) \right] e$$

where  $\alpha$  is the learning rate in [Tables S1](#) and [S2](#). Under a greedy policy, the model-free agent at decision time will choose the action  $a$  in state  $s$  with the highest state-action value  $Q(s, a)$ . If multiple actions with the same maximal value exist, then the agent samples from these with equal probability. The eligibility trace  $e$  is set to zero at the beginning of each trial. Example trajectories can be seen in [Video S3](#).

### Model-based agent

The model-based agent is provided with an internal 10x10 binary grid representation of which maze modules are present or not in the environment. Every state  $s$  in the agent's model  $\chi$  corresponds a module in the maze (see [Figures 1A](#) and [1B](#)); as it transitions through the environment, it updates the internal model at every timestep according to the adjacent states  $s'$ .

$$\chi(\mathbf{s}') \leftarrow \begin{cases} 1 & \text{if module } \mathbf{s}' \text{ is present} \\ 0 & \text{if module } \mathbf{s}' \text{ is missing} \end{cases}$$

At decision time, the model-based agent uses its model  $\chi$  and to plan the shortest route to the goal from each possible next state. Shortest routes were calculated using an A\* tree search algorithm.<sup>120</sup> In the event of multiple equally short routes to the goal, their respective actions were sampled with equal probability. Example trajectories can be seen in [Video S4](#).

### Successor representation agent

The SR somewhat combines parts of model-free and model-based learning<sup>60,61</sup> by using experience to learn a predictive map  $M$  between the states in an environment. For a one-step state transition matrix  $T$ , the predictive map is equivalent to the discounted sum of future state transitions:

$$M = I + \gamma T + \gamma^2 T^2 + \dots = \sum_{t=0}^{\infty} \gamma^t T^t$$

This discounting of transitions means  $M$  can be readily combined with a separately learned reward  $R$  associated with each state  $s$  in order to explicitly compute value.

$$V(s) = \sum_{s'} M(s, s') R(s')$$

The SR agent uses temporal-difference learning and eligibility traces to update the successor matrix  $M$ .<sup>121</sup> After transitioning from state  $s_t$  and to state  $s_{t+1}$ , the agent will first decay its eligibility trace  $e$  - a vector with length equal to the number of states in the environment:

$$e \leftarrow \lambda \gamma e$$

where  $\lambda = 0.5$  is the eligibility trace decay parameter and  $\gamma$  is the discount factor of the value function in [Tables S1](#) and [S2](#). Next, the successor representation agent will update its eligibility trace:

$$e(\mathbf{s}_t) \leftarrow e(\mathbf{s}_t) + 1$$

before finally updating the successor representation.<sup>121</sup>

$$M \leftarrow M + \alpha [\mathbb{1}_{st} + \gamma M(\mathbf{s}_{t+1}, :) - M(\mathbf{s}_t, :)] \otimes e$$

where  $\otimes$  indicates an outer product. This can then be combined with the state-rewards  $R$  at decision time to compute the value of prospective future states.

$$R(s) = \begin{cases} 1 & \text{if } s \text{ is the goal} \\ 0 & \text{otherwise} \end{cases}$$

Under a greedy policy, the successor representation agent at decision time will choose the next available state with the highest value. If multiple available states exist with equally high values, then the agent samples from these with equal probability. The eligibility trace  $e$  is set to zero at the beginning of each trial. Example trajectories can be seen in [Video S5](#).

## QUANTIFICATION AND STATISTICAL ANALYSIS

Optimal paths were calculated using the A\* tree search algorithm<sup>120</sup> in the 10x10 grid state space, with path length measured in terms of state visitations. Occupancy correlations were calculated using the Pearson correlation between the proportion of time spent in each state of the 10x10 grid state space. One- and two-sample t-tests were implemented using MATLAB's `ttest` and `ttest2` functions.

Likelihoods were calculated by inputting individual human/rat state trajectories to the RL agents and calculating the internal value estimates of the available state transitions conditional on the human/rat's past trajectories. These value estimates were used in a softmax function to calculate at each time point, the probability that the agent would take each of the available actions conditioned

on the human/rat's past. Maximum likelihood parameters were estimated using MATLAB's `fmincon` function to minimise the negative log-likelihood.

Mahalanobis distances were calculated using MATLAB's `pdist2` function on the diffusivity metrics for the humans, rats, model-free, model-based and successor representation agents.

The minimum path distance analysis used an individual human/rat trajectory as a reference trajectory. At each time point along that trajectory, the A\* tree search algorithm<sup>120</sup> was used to find the shortest path distance on the maze configuration to the agent trajectories trained from that individual human/rat's behaviour. Averaging along the length of the trajectory then gives a measure of similarity between that reference trajectory and the simulated agents.

**Current Biology, Volume 32**

**Supplemental Information**

**Predictive maps in rats and humans**

**for spatial navigation**

**William de Cothi, Nils Nyberg, Eva-Maria Griesbauer, Carole Ghanamé, Fiona Zisch, Julie M. Lefort, Lydia Fletcher, Coco Newton, Sophie Renaudineau, Daniel Bendor, Roddy Grieves, Éléonore Duvelle, Caswell Barry, and Hugo J. Spiers**



**Figure S1: The maze environment used for the rat experiment, related to Figure 1.** The environment consists of 100 removable maze modules with a black curtain over one of the surrounding edges to provide a single extra-maze cue. Reward can be dispensed at the goal module by filling the well with chocolate milk via polymeric tubing beneath the maze.

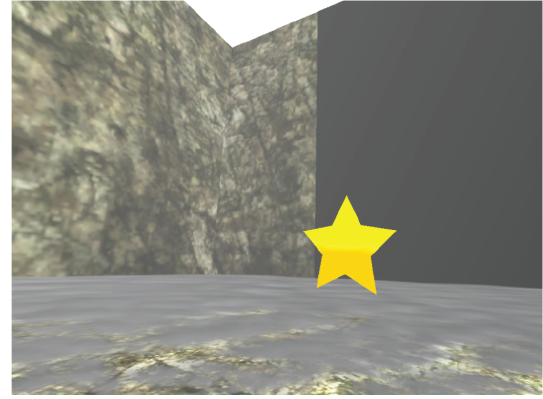
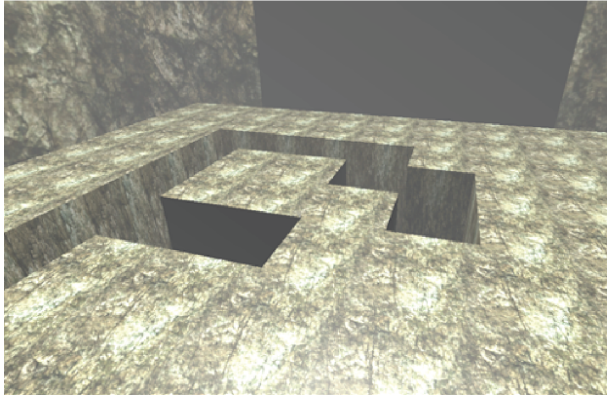


**Figure S2: The virtual environment used for the human experiment, related to Figure 1.** The environment had the same proportions as the rat environment and consisted of 100 removable mazes modules with a black curtain over one of the surrounding edges to provide a single extra-maze cue. A seamless texture was applied to the maze modules and walls and a fog lined the floor of the maze (see right image) to ensure humans had to rely on spatial memory to understand the maze structure. Reward was indicated by a gold star that would appear at the goal module when the participant successfully navigated to it.

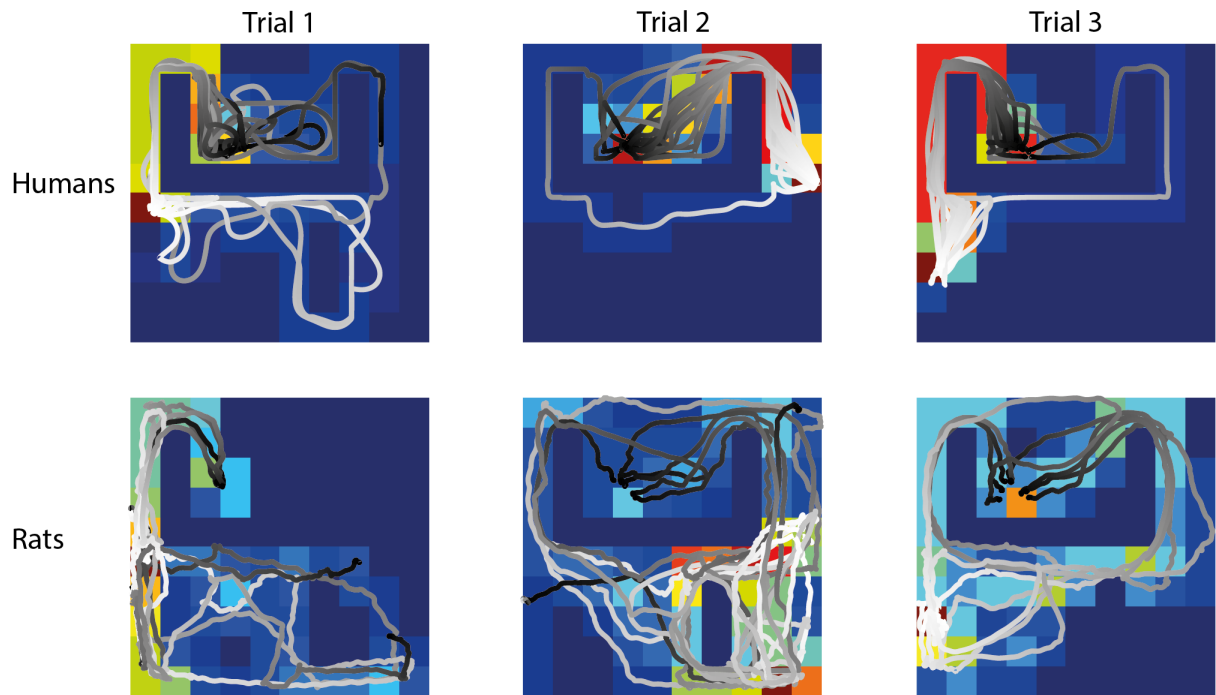


**Figure S3: The route choices of humans and rats were often suboptimal at the start of a new maze configuration, related to Figure 2.** Examples of the human (top) and rat (bottom) trajectories overlaying occupancy maps for the first 3 trials on maze configuration 20. The white-black colour gradient shows the beginning-end of each trajectory. Initially the paths taken by the humans and rats were often suboptimal (leftmost column) with performance generally improving rapidly within the first 3 trials of a new maze configuration. The goal location is 4 squares right and down from the top-left corner.



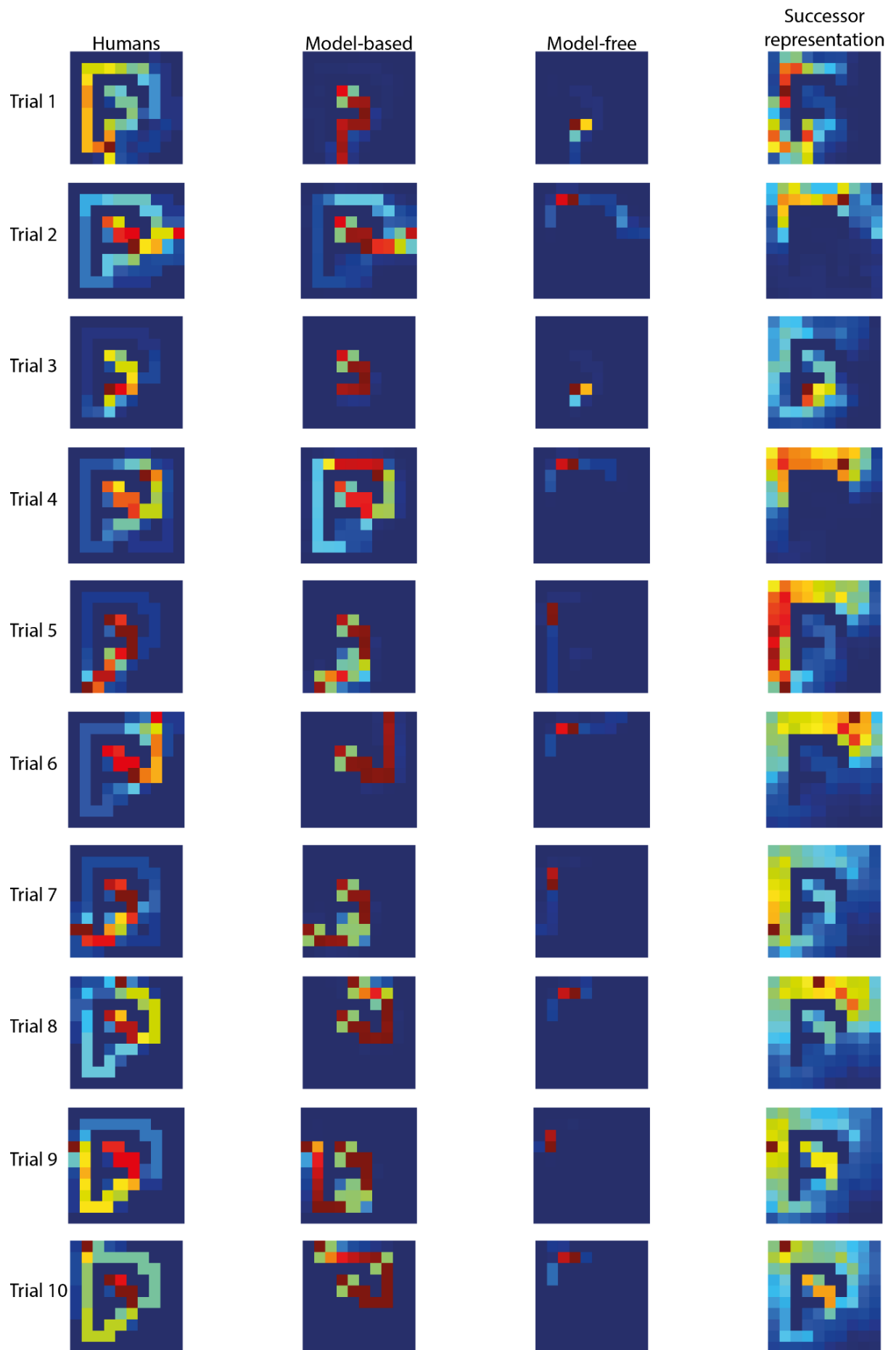


**Figure S4: Human and agent occupancy maps for maze configuration 21, related to Figure 6.** The occupancy maps of the humans (leftmost column) and agents for each of the 10 trials (rows) on maze configuration 21. The Model-Based agent (second column) quickly learns an accurate model of the environment and uses it to choose the shortest route to the goal with respect to that model (goal location is 4 squares right and down from the top-left corner). Conversely, the model-free agent (third column) is unable to update its value representation fast enough to successfully adapt to the new maze configuration, and particularly struggles on later trials where the starting position requires longer and more tortuous routes. The successor representation agent (rightmost column) sits on the spectrum between model-based and model-free methods, initially struggling to find an efficient route to the goal but providing a good match to the human behaviour on later trials.

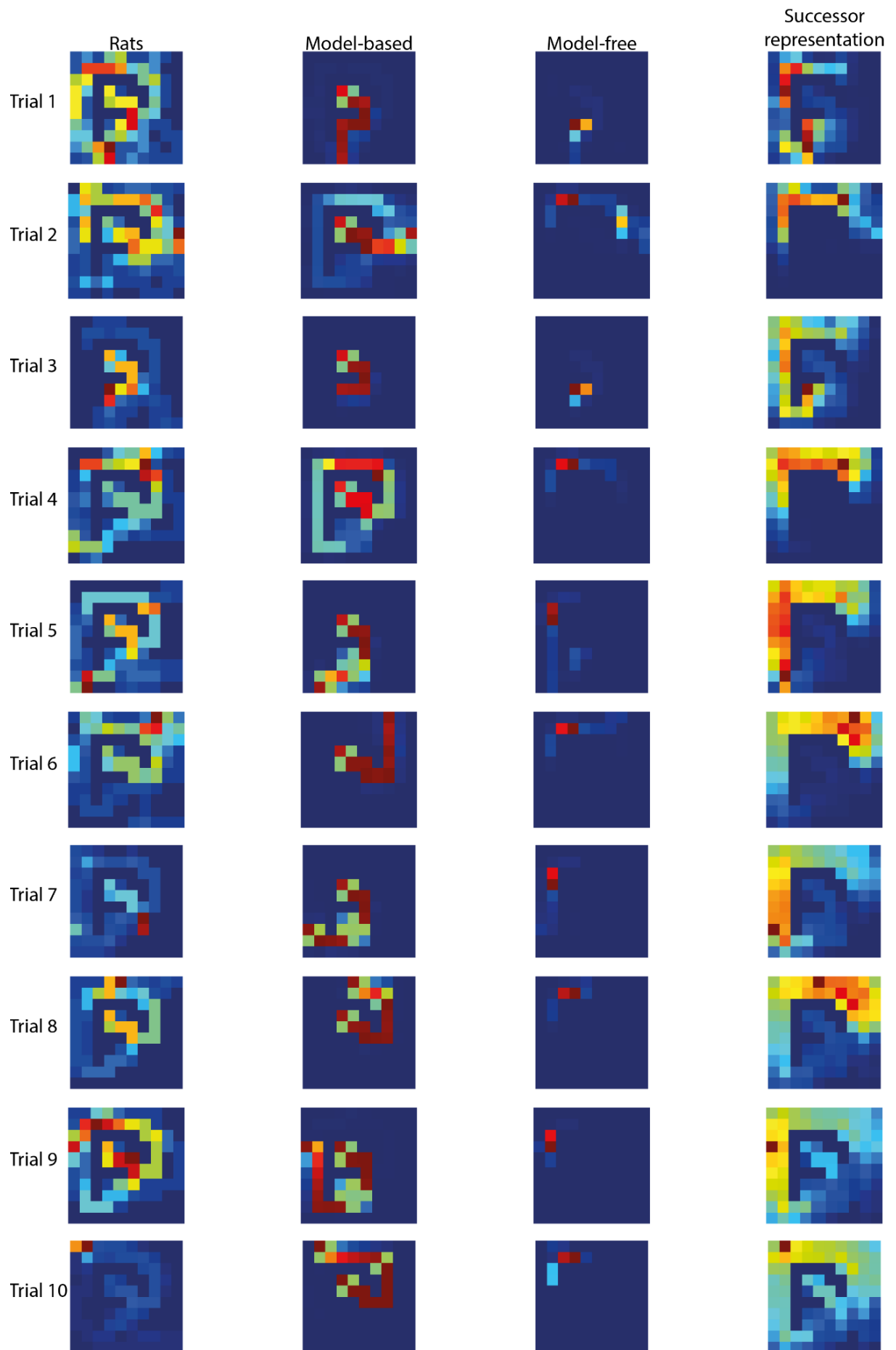


**Figure S5: Rat and agent occupancy maps for maze configuration 21, related to Figure 6.** The occupancy maps of the rats (leftmost column) and agents for each of the 10 trials (rows) on maze configuration 21. The Model-Based agent (second column) quickly learns an accurate model of the environment and uses it to choose the shortest route to the goal with respect to that model (goal location is 4 squares right and down from the top-left corner). Conversely, the model-free agent (third column) is unable to update its value representation fast enough to successfully adapt to the new maze configuration, and particularly struggles on later trials where the starting position requires longer and more tortuous routes. The successor representation agent (rightmost column) sits on the spectrum between model-based and model-free methods, initially struggling to find an efficient route to the goal but providing a good match to the rat behaviour on later trials.

Agent	$\alpha$			$\gamma$		
	MF	MB	SR	MF	MB	SR
Participant 1	0.09	1	1	0.43	0.80	0.76
Participant 2	0.08	1	0.89	0.43	0.80	0.79
Participant 3	0.11	1	1	0.51	0.81	0.82
Participant 4	0.30	1	0.96	0.62	0.82	0.81
Participant 5	0.07	1	0.80	0.41	0.80	0.77
Participant 6	0.11	1	0.81	0.60	0.82	0.85
Participant 7	0.07	1	1	0.40	0.79	0.78
Participant 8	0.15	1	1	0.54	0.80	0.77
Participant 9	0.09	1	0.93	0.50	0.80	0.77
Participant 10	0.19	1	0.82	0.64	0.83	0.84
Participant 11	0.11	1	0.92	0.54	0.81	0.78
Participant 12	0.16	1	0.98	0.55	0.80	0.75
Participant 13	0.12	1	1	0.52	0.80	0.77
Participant 14	0.12	1	0.94	0.51	0.80	0.76
Participant 15	0.14	1	0.78	0.56	0.80	0.75
Participant 16	0.13	1	1	0.59	0.81	0.80
Participant 17	0.13	1	0.77	0.62	0.82	0.85
Participant 18	0.19	1	0.91	0.55	0.80	0.75

**Table S1: Human behaviour maximum likelihood parameters, related to Figure 3.** The learning rates  $\alpha$  and discount factors  $\gamma$  for the model-free (MF), model-based (MB) and successor representation (SR) agents, calculated for each individual.

Agent	$\alpha$			$\gamma$		
	MF	MB	SR	MF	MB	SR
Rat 1	0.07	1	0.76	0.43	0.79	0.80
Rat 2	0.11	1	0.77	0.48	0.80	0.83
Rat 3	0.12	1	0.87	0.45	0.79	0.71
Rat 4	0.65	1	0.87	0.01	0.78	0.76
Rat 5	0.42	1	0.77	0.01	0.78	0.77
Rat 6	0.09	1	0.90	0.34	0.79	0.79
Rat 7	0.12	1	0.70	0.16	0.80	0.82
Rat 8	0.08	1	0.91	0.28	0.78	0.81
Rat 9	0.07	1	0.87	0.42	0.80	0.81

**Table S2: Rat behaviour maximum likelihood parameters, related to Figure 3.** The learning rates  $\alpha$  and discount factors  $\gamma$  for the model-free (MF), model-based (MB) and successor representation (SR) agents, calculated for each individual.